MAGNETIC RESONANCE IN CHEMISTRY
Magn. Reson. Chem. 2004; **42**: S138–S157
Published online in Wiley InterScience (www.interscience.wiley.com). DOI: 10.1002/mrc.1452

Systematic strategy for decoding the NMR spin–spin coupling mechanism: the J-OC-PSP method†

Jürgen Gräfenstein and Dieter Cremer*

Department of Theoretical Chemistry, Göteborg University, Reutersgatan 2, S-41320 Göteborg, Sweden

Received 12 February 2004; Revised 11 May 2004; Accepted 11 May 2004

Criteria for analyzing the NMR spin–spin coupling mechanism were derived. Advantages and disadvantages of parallel- and post-processing analytical methods are discussed. An orbital decomposition into just one-orbital contributions provides less information than a decomposition into one-, two- and *m*-orbital effects. If just the last orbital in an orbital path leading from the perturbing to the responding nucleus is considered, the physics of the transport of spin information cannot be described. The theory of the J-OC-PSP (decomposition of *J* into *O*rbital *C*ontributions using *O*rbital *C*urrents and *P*artial *S*pin *P*olarization) is described to demonstrate the role of orbital contributions, orbital spin densities and orbital currents for the coupling mechanism. J-OC-PSP1 provides a decomposition into one- and two-orbital contributions with distinct physical reference (Ramsey perturbation of orbitals, steric exchange interactions, etc.) whereas J-OC-PSP2 introduces distinct orbital paths from perturbing to responding nucleus, clarifies the difference between active, passive and frozen orbitals and makes it possible to separate through-space from through-bond spin–spin coupling mechanism. Fermi contact coupling in hydrocarbons over more than two bonds is found to occur preferentially through space by tail interactions of the orbitals, as was anticipated in the early work of Barfield.

KEYWORDS: NMR; spin–spin coupling mechanism; J-**OC**-PSP

INTRODUCTION

The elucidation of the NMR spin–spin coupling mechanism has a long history because it is directly connected with the need to predict and understand the sign and magnitude of measured spin–spin coupling constants (SSCCs).[1] Ramsey described the physics of the spin–spin coupling mechanism and this description is still valid today.[2] Early work clarified the important role of the Fermi contact (FC) contribution to the SSCC. The dependence of the FC term and hence of the SSCC on geometric features was recognized and its analysis was highlighted in the seminal work of Karplus, who used valence bond theory to unravel the relationship between the magnitude of vicinal SSCCs and the dihedral angle defined by the major spin–spin coupling path.[3,4] Barfield and Karplus[5] related the FC term of the SSCC to fragment bond orders and were the first to distinguish between direct and indirect bond contributions to the coupling path. We will show later that this is the origin for distinguishing between active and passive orbital contributions (the terms direct and indirect are used nowadays in a different fashion[1]). Later, LCAO-MO descriptions were given[6] that provided a true alternative to the valence bond (VB) descriptions of the spin–spin coupling mechanism. In this way, inductive and hyperconjugative effect of substituents on the SSCC were rationalized.[7]

The early work on the spin–spin coupling mechanism focusing on the FC term was nicely summarized by Barfield and Chakrabarti.[8] A distinction between through-bond and through-space coupling mechanisms was made.[9] In this connection, Barfield and co-workers pointed out the importance of back-lobe interactions.[10] Describing, for example, the framework of bonds in a C_{2v}-symmetrical propane unit by localized MOs (LMOs), the back lobes of the in-plane CH bond orbitals in the 1,3-position can overlap through space and hence facilitate the transport of spin information from the in-plane H(C1) proton to the in-plane H(C3) proton.[8,10] The effect of the back-lobe interactions is the fundamental principle of long-range couplings in σ-systems with an all-*trans* ('zig-zag' or 'W') conformations.[8,10,11] Through-bond and through-space effects and active and passive LMO ('direct and indirect') contributions work together to lead to SSCC over four, five or more bonds.[8]

Barfield and Sternhels demonstrated also the importance of π-orbitals for the FC spin–spin coupling mechanism for homoallylic coupling[12] and the coupling in cumulenes and conjugated polyenes.[8] Barfield and co-workers discussed different coupling paths through the π-system and the practical limits of long-range coupling. They also investigated multi-path coupling[13] and the coupling mechanism via H-bonds in proteins.[14] By investigating the steric requirements for the various coupling paths, the measured SSCC became an

†Dedicated to Professor M. Barfield on the occasion of his 70th birthday.

*Correspondence to: Dieter Cremer, Department of Theoretical Chemistry, Göteborg University, Reutersgatan 2, S-41320 Göteborg, Sweden. E-mail: dieter.cremer@theoc.gu.se

important tool for structure elucidation in the solution phase, for which other methods of structural analysis provide little information.

The early work on the spin–spin coupling mechanism focused almost exclusively on FC coupling, although the physics of three other coupling terms (DSO, diamagnetic spin–orbit; PSO, paramagnetic spin–orbit; and SD, spin–dipole term) was well understood since Ramsey.[2] The reason for this preference had, of course, to do with the fact that (a) for many SSCCs in organic molecules the FC dominates and (b) for a long time finite perturbation theory (FPT)[15] was the method of choice to calculate just the FC term so that theory mostly did not consider the non-contact (NC) terms DSO, PSO and SD.[16] Today, the accepted standard is to calculate all four Ramsey terms.[17–23]

With the improved possibilities of calculating NMR SSCCs, the investigation of the spin–spin coupling mechanism experienced a renaissance, which was initialized by a number of review articles by Contreras and co-workers.[24–26] They used the large repertoire of measured and calculated SSCCs collected in the first four to five decades of NMR spectroscopy to describe a number of stereoelectronic effects influencing the spin–spin coupling mechanism. They also suggested several methods to decompose calculated SSCCs into orbital contributions and therefore we will frequently refer to his work.[27–29]

In this paper, we will exclusively consider SSCCs calculated with coupled-perturbed density functional theory (CP-DFT) to analyze the spin–spin coupling mechanism.[22,23] Although there are also wavefunction- rather than density-based ways of calculating SSCCs,[17–21] we consider CP-DFT advantageous in this connection for the following reasons: (a) CP-DFT carried out with a standard GGA (general gradient approximation)[30] or hybrid exchange-correlation functional[31] accounts for not only dynamic but also non-dynamic correlation effects, which are indirectly incorporated via the local character of the exchange functional and the resulting self-interaction error.[32–35] In this way, the singlet–triplet (quasi-)instability problems accompanying the calculation of the FC part of an SSCC are largely suppressed. (b) Basis set truncation errors are less serious for DFT methods than for wavefunction theory (WFT) methods.[32] This makes it easier to set up basis sets for SSCC calculations.[36] (c) The spin–spin coupling mechanism is strongly driven by exchange interactions. DFT provides the possibility of fine-tuning the exchange functional so that fairly accurate SSCCs are obtained.[22] (d) An important aspect of all SSCC calculations is the cost factor. A CP-DFT calculation of an SSCC is less costly than a WFT calculation of the SSCC. Therefore, the magnetic properties of large molecules relevant for experimental studies can be investigated with CP-DFT at a high level of accuracy (given by basis set and XC-functional).[37–41] (d) Directly related to point (c) is the mode of analysis of the SSCC, which we will pursue in this work. This may imply repeated calculations of the SSCC or its parts, which can be easily carried out if the method used is not too costly.[42–50]

Utilizing CP-DFT, we will discuss the pros and cons of the various ways of elucidating the spin–spin coupling mechanism. There is no unique way of analyzing an SSCC because its four Ramsey terms and the orbital contributions to the Ramsey terms are not observable quantities and therefore are only defined within a given model. The usefulness of the model, however, will be reflected by the physical basis of the mechanistic description resulting therefrom. Therefore, a given way of decomposing, analyzing and interpreting the spin–spin coupling mechanism can only be judged according to (a) the theoretical soundness of its derivation, (b) the ease of applying it, (c) the scientific value of its results and (d) the physical consistency of the latter. Effects identified with a given analysis of the SSCC, which contradict physical laws or chemical knowledge, are strong evidence for an ill-defined analysis model for the SSCCs.

In the next section, we present and discuss the repertoire of tools available for analyzing the spin–spin coupling mechanism as it is available in the two levels of the J-**OC**-PSP (decomposition of *J* into *O*rbital *C*ontributions using *O*rbital *C*urrents and *P*artial *S*pin *P*olarization: J-OC-OC-PSP = J-**OC**-PSP) approach, namely J-**OC**-PSP1[42] and J-**OC**-PSP2.[43] In the third section, the application of these approaches to typical SSCCs is demonstrated and the outcome compared with those of other orbital decomposition methods. Finally, in the fourth section, we give a systematic overview over criteria that should be fulfilled by an analysis of SSCCs. We discuss the extent to which J-**OC**-PSP fulfills these criteria and suggest general guidelines for the application of J-**OC**-PSP.

THEORETICAL BASIS AND COMPUTATIONAL DETAILS

The investigation and analysis of the NMR spin–spin coupling mechanism with the help of theoretical tools depends on what method is used to calculate SSCCs. This could be with FPT[15] using various types of WFT (Hartree-Fock, second-order many-body perturbation theory,[51] configuration interaction,[52] MCSCF,[53] coupled cluster theory,[54] etc.) or DFT methods.[55–59] Alternatively, coupled perturbed theory could be used at the Hartree–Fock (HF),[60,61] MCSCF,[19] second-order polarization propagator approximation (SOPPA),[18] equation of motion coupled cluster (EOM-CC),[20] projected coupled cluster with all single and double excitations (CCSD)[21] or DFT level of theory.[22,23] We chose CP-DFT because many of the terms that we define in the following for analyzing the coupling mechanism are easily available at this level of theory.

Also, it is not a trivial question to ask what kind of orbitals are used for the analysis. Best suited are localized molecular orbitals (LMOs), because they make it possible to formulate the results of the orbital analysis in a familiar chemical language. LMOs lead to core, bond and lone pair orbitals, which facilitate distinguishing between the effects of core and valence orbitals,[42] specifying lone pair effects[42] or relating the spin transport along a given orbital path to a particular bond path.[48] Clearly, the magnitude of a given orbital contribution will change with the choice of the orbitals [Boys LMOs,[62] natural localized molecular orbitals (NLMOs),[63] canonical orbitals, etc.]; however, if a particular effect of the spin–spin coupling mechanism is identified for one type of orbital, its physical significance can be verified by testing whether another choice of orbital leads to the same effect.

A third question concerns whether the analysis of the SSCC is carried out after (*post-processing methods*) or during its calculation (*parallel-processing methods*). This is not a trivial question because cost considerations favor the first choice, but this limits significantly the possibilities of the analysis. Because of this, the J-**OC**-PSP methods discussed in this work are parallel-processing methods in the sense that the status of the individual orbitals (active, passive or frozen) has to be taken into account in the SSCC calculation from the beginning. This is in contrast to a post-processing method, where the orbital analysis is performed after a standard SSCC calculation. We will consider both possibilities in this work and compare their pro and cons.

Also, it has to be clarified whether the SSCC and their Ramsey terms are decomposed into just one-orbital contributions, one- and two-orbital contributions or one-, two- and *n*-orbital contributions. One could argue that a one-orbital analysis is appropriate because the four Ramsey terms are all one-electron quantities. However, this suppresses an important part of the spin–spin coupling mechanism transporting information between two coupling nuclei with the inclusion of many electrons. Hence the more detailed the orbital decomposition carried out, the more detailed the spin–spin coupling mechanism can be described. We will begin by sketching the theory of the J-**OC**-PSP methods, which can function as either one-, two- or *n*-orbital methods.[42–50]

Any analysis method should consider the total spin–spin coupling mechanism leading from the perturbing to the responding nucleus. An approach which considers just the changes in the zeroth-order density at the responding nucleus (or perturbing nucleus) is inferior to a complete description of the spin–spin coupling mechanism.

A simple requirement for any analysis method that decomposes the SSCC into orbital contributions is that this method must also be applicable to each of the four Ramsey terms and that the sum of the orbital contributions must add up to the total SSCC or the Ramsey terms.

Although the orbital contributions to the SSCC will depend on the orbitals used for the analysis, it is undesirable that any of the orbital contributions depends on the choice of the perturbing nucleus for a given SSCC. An exchange of perturbing and responding nucleus must lead to the same orbital contribution (*nuclear independence*) considering the micro-reversibility of the spin–spin coupling mechanism.

One- and two-orbital mechanisms in spin–spin coupling. The J-OC-PSP methods

The calculation of an SSCC between coupling nuclei A and B carried out by CP-DFT is described in detail elsewhere.[22] For each of the first-order Ramsey terms (i.e. PSO, FC and SD terms; DSO is a zeroth-order term), the nuclear magnetic moment at the perturbing nucleus B gives rise to first-order changes of the Kohn–Sham (KS) orbitals.[64] These changes in turn generate a magnetic field at the site of the responding nucleus A, which will be sensed by the nuclear magnetic moment at A. Each of the three first-order Ramsey terms is given by

$$K_{\mathrm{AB}}^{X} = \sum_{k}^{\mathrm{occ}} \underbrace{\langle \psi_k^{(B),X} | h^{(A),X} | \psi_k^{(0)} \rangle}_{= K_{\mathrm{AB}}^{X,k}} \tag{1}$$

where K_{AB}^{X} is the reduced SSCC between nuclei A and B split up in the first-order Ramsey terms X = PSO, FC, SD. The symbol $h^{(A),X}$ denotes the operator for the electron–nuclear spin interaction according to term X at nucleus A, $\psi_k^{(0)}$ the unperturbed KS orbitals and $\psi_k^{(B),X}$ the first-order KS orbitals resulting from a perturbation with the operator $h^{(B),X}$ (perturbation at nucleus B). In the following, we will omit the superscript X. Further, we will make no difference between spin and space orbitals. We consider closed-shell systems, which means that the first-order space orbitals corresponding to a pair of α and β zeroth-order orbitals are equal for the PSO term and opposite for the FC and SD terms. The first-order orbitals $|\psi_k^{(B)}\rangle$ are given by the integral

$$\langle \psi_a^{(0)} | \psi_k^{(B)} \rangle = \frac{\langle \psi_a^{(0)} | F^{(B)} | \psi_k^{(0)} \rangle - \sum_{l,l\neq k} F_{kl}^{(0)} \langle \psi_a^{(0)} | \psi_l^{(B)} \rangle}{F_{kk}^{(0)} - \varepsilon_a} \tag{2}$$

Here and in the following, indices $\{k, l, m\}$ denote occupied, index $\{a\}$ virtual and indices $\{p, q\}$ arbitrary orbitals. The symbol $F_{kl}^{(0)}$ denotes the zeroth-order KS matrix elements and ε_a is the energy of orbital a. For a derivation of Eqn (2), see Ref. 43.

Equations (1) and (2) are valid for both canonical and non-canonical occupied orbitals. In the first case, the numerator and denominator on the right-hand side of Eqn (2) simplify in so far as $F_{kk}^{(0)}$ is replaced by ε_k and the second term of the numerator vanishes because all $F_{kl}^{(0)} = 0$ for $l \neq k$. As mentioned above, the use of LMOs is advantageous for mechanistic studies of SSCCs and, in the following, orbitals $|\psi_k^{(0)}\rangle$ denote LMOs unless stated otherwise.

The first-order KS operator $F^{(B)}$ consists of $h^{(B)}$ and a contribution $\tilde{F}^{(B)}$ that covers the feedback of the first-order orbitals to the KS operator, i.e. $F^{(B)}$ accounts for the electron–electron interactions triggered by the magnetic perturbation. One can decompose $F^{(B)}$ into contributions from individual orbitals:

$$\hat{F}^{(B)} = \hat{H}^{(B)} + \hat{\tilde{F}}^{(B)} \tag{3a}$$

$$\hat{\tilde{F}}^{(B)} = \sum_{l} \hat{\tilde{F}}_l^{(B)} \tag{3b}$$

$$\hat{\tilde{F}}_l^{(B)} = \int \mathrm{d}^3 r \frac{\delta \hat{F}}{\delta \psi_l^{(0)}} \psi_l^{(B)}(\mathbf{r}) \tag{3c}$$

Equations (3a–c) refer to the KS operator and its components as a whole, not to individual components, which is indicated by a circumflex. In CP-DFT in general, $\tilde{F}^{(B)}$ describes changes in the Coulomb interaction in addition to exchange and correlation effects. For a magnetic perturbation, the electron density and therefore the Coulomb interaction remains unchanged in first order, i.e. $\tilde{F}^{(B)}$ cannot contain any Coulomb effects. As exchange effects are usually much larger than

correlation effects, $\tilde{F}^{(B)}$ describes in first order self-exchange and exchange-interaction effects between the orbitals.

By inserting Eqn (3a) into Eqn (2), one obtains

$$C_{ak}^{(B)} = \frac{1}{F_{kk}^{(0)} - \varepsilon_a}\left[h_{ak}^{(B)} + (\tilde{F}_k^{(B)})_{ak} + \sum_{l,l\neq k}\left((\tilde{F}_l^{(B)})_{ak} - F_{kl}^{(0)}C_{al}^{(B)}\right)\right] \quad (4)$$

Here, matrix elements of the form $\langle\psi_p^{(0)}|\cdots|\psi_q^{(0)}\rangle$ are denoted with the index pair pq and $C_{ak}^{(B)} = \langle\psi_a^{(0)}|\psi_k^{(B)}\rangle$.

The terms in the square brackets in Eqn (4) correspond to the different mechanisms that can lead to a perturbation of orbital k: $h^{(B)}$ describes the direct response of orbital k to the external perturbation, i.e. the Ramsey perturbations. The term $\tilde{F}_k^{(B)}$ covers the enhancement of this perturbation by feedback effects in the orbital k itself. For the FC term, this feedback is easy to rationalize by exchange effects: The perturbation by $h_{ak}^{(B)}$ leads to opposite changes in the α and β orbitals and therefore to an energetically favorable decrease of the $\alpha-\beta$ orbital overlap (optimization of exchange interactions), and eventually to an increase of the spin polarizability of orbital k. The last two terms describe changes in orbital k caused by changes in orbital l, which arise by two essentially different mechanisms:

1. If orbital l undergoes a change in response to the Ramsey perturbation, then orbital k will reoptimize its exchange interaction with l. This effect is described by $\tilde{F}_l^{(B)}$. It is related to the classical chemical concept of steric repulsion and will therefore be denoted *steric exchange interaction*.
2. The one-particle energy of an LMO is not stationary under all small changes of the LMO but only for such changes that do not violate the orthogonality between the occupied LMOs. Hence, if orbital l responds to the perturbation by an excitation into a and l becomes partly unoccupied, the one-particle energy of orbital k can be decreased by a delocalization $k \rightarrow l$, which has to be accompanied by an excitation $k \rightarrow a$ to maintain orthogonality between orbitals k and l. This process is described by the term $\sum_{l,l\neq k} F_{kl}^{(0)}C_{al}^{(B)}$ in Eqn (4). It can be regarded as a *resonance interaction* between orbitals k and l and does not include any dynamic electron correlation interactions between the electrons in orbitals k and l. For canonical orbitals, the $F_{kl}^{(0)}(l \neq k)$, and hence the resonance term, become zero as canonical orbitals are already delocalized.

There is an important difference between the classical steric repulsion and the steric exchange interaction discussed under (1): if two molecular fragments approach each other, the geometry and hence the orbitals will be distorted. The orthogonality between the occupied orbitals, i.e. the Pauli principle, will be violated and has to be restored by a readjustment of the orbitals involved. In the case of a magnetic perturbation (accompanying spin–spin coupling), the geometry of the molecule is unaffected and there is no violation of orthogonality: an excitation $l \rightarrow a$ does not affect the orthogonality between k and l in first order. Hence the steric exchange interaction is not driven by a violation of the Pauli principle but implies a pure energy reoptimization. There have been misconceptions in this point in the literature.[65]

Equation (4) describes changes of orbital k triggered both directly by $h^{(B)}$ and by changes in orbital l. However, the changes in orbital l are in turn caused both by $h^{(B)}$ directly and by changes in a third orbital m, etc. In other words, the transfer of spin information from nucleus B to A may take place through orbital paths of arbitrary length, which may contain the same orbital several times. For instance, the following paths will occur:

$$(\mathrm{B}) \rightarrow k \rightarrow (\mathrm{A}) \quad (5a)$$

$$(\mathrm{B}) \rightarrow k \rightarrow l \rightarrow (\mathrm{A}) \quad (5b)$$

$$(\mathrm{B}) \rightarrow k \rightarrow l \rightarrow m \rightarrow (\mathrm{A}) \quad (5c)$$

$$(\mathrm{B}) \rightarrow k \rightarrow l \rightarrow k \rightarrow (\mathrm{A}) \quad (5d)$$

$$(\mathrm{B}) \rightarrow k \rightarrow l \rightarrow l \rightarrow (\mathrm{A}) \quad (5e)$$

$$(\mathrm{B}) \rightarrow k \rightarrow l \rightarrow l \rightarrow k \rightarrow (\mathrm{A}) \quad (5f)$$

$$(\mathrm{B}) \rightarrow k \rightarrow l \rightarrow l \rightarrow k \rightarrow k \rightarrow (\mathrm{A}) \quad (5g)$$

The orbitals within a path play different roles in the transfer of spin information:

1. The first orbital in a path receives the spin interaction directly from nucleus B and passes it either directly to nucleus A or (by steric exchange or resonance interaction) to another orbital.
2. The last orbital in a path passes spin information directly to nucleus A. For paths containing only one step, as in Eqn (5a), (1) and (2) coincide.
3. All other orbitals do not interact directly with any nucleus but act as an intermediate link in the transition of spin information.

Orbital contributions to the SSCC according to points (1) and (2) are called *active contributions* and those according to (3) *passive contributions*.[43] Correspondingly, an orbital that makes any active contributions to the spin information transfer is called an *active orbital*, whereas orbitals that exclusively act according to (3) are denoted *passive orbitals*. Note that an active orbital usually makes both an active and a passive contribution to the spin–spin coupling [see Eqns (5e) and (5g)].

One-orbital descriptions

The decomposition of the total spin coupling mechanism into orbital paths is a useful starting point for orbital decompositions of SSCC terms. A simple decomposition of the SSCC into one-orbital contributions is given by Eqn (1). The orbital contributions K_{AB}^k comprise all orbital paths where k occurs as *last orbital* before nucleus A, i.e. the decomposition is done from the viewpoint of the responding nucleus A. Such a decomposition is a computationally cheap way to gain a first insight into the spin–spin coupling mechanism. However, it is limited in two ways: (a) it allows no distinction between one- and two-orbital mechanisms; (b) it is not symmetric with respect to perturbing and responding nucleus. The natural *J*-coupling (NJC) approach suggested by Peralta *et al*.[29] (henceforth called NJC-1) decomposes the FC term in the spirit of Eqn (1) in connection with NLMOs[63] and FPT.[15]

One- and two-orbital descriptions

The notion of active and passive orbital contributions allows for a decomposition of the SSCC into one- and two-orbital contributions that is symmetric with respect to A and B. In the J-**OC**-PSP1 approach,[42] all orbital paths where orbital k is active with respect to both A and B are summed in the one-orbital contribution $K_{AB}^{PSP1}(k)$ (PSP1 as short form for J-**OC**-PSP1) and all contributions where both orbitals k and $l (k \neq l)$ act as active orbitals are summed up in the contribution K_{AB}^{PSP1} $(k \leftrightarrow l)$. Here, the notation $(k \leftrightarrow l)$ indicates both the interaction between orbitals k and l and the symmetry with respect to interchanges $k \leftrightarrow l$ as well as $A \leftrightarrow B$. In cases where three- and more-orbital paths play only a minor role (e.g. one-bond SSCCs in small molecules[42]), J-**OC**-PSP1 provides a decomposition of the SSCC into one- and two-orbital terms that corresponds well with the underlying one- and two-electron mechanisms of NMR spin–spin coupling.

The J-**OC**-PSP1 orbital contributions can be calculated by modified SSCC calculations where one or more orbitals are forcibly set passive. This means that the coupling between these orbitals and the operators $h^{(A)}$, $h^{(B)}$ is put to zero, i.e.

$$h_{ak}^{(N),\mathrm{pass}} = \sum_{a'k'} \left(\delta_{aa'}\delta_{kk'} - P_{ak,a'k'}^{\mathrm{pass}}\right) h_{ak}^{(N)} \tag{6a}$$

(N = A, B), where

$$P_{ak,a'k'}^{\mathrm{pass}} = \begin{cases} 1 \text{ for } a = a', k = k', k \text{ passive} \\ 0 \text{ otherwise} \end{cases} \tag{6b}$$

projects out those orbitals that are to be set passive. As has been shown,[43] a complete J-**OC**-PSP1 decomposition can be performed with a series of calculations according to Eqns (6a) and (6b) where one orbital is kept active whereas all other orbitals are set passive.

One-, two- and n-orbital descriptions

In several cases, passive orbitals play an important role for the transmission of the spin information. For example, the groups of Barfield,[8,11] Contreras,[27,66] Fukui[67] and others[68] showed that the π system in polyenes plays an important role in the FC coupling mechanism and dominates the value of the long-range SSCCs in conjugated molecules. J-**OC**-PSP1 does not make it possible to identify these contributions and, instead, distributes them over the one- and two-orbital terms. The J-**OC**-PSP2 approach[43] determines contributions from orbital paths with any number of orbitals involved. Orbital contributions are classified as arising from both active and passive rather than just active orbitals in the coupling path. That is, the contribution $K_{AB}^{PSP2}(k)$ includes all orbital paths to which orbital k contributes, $K_{AB}^{PSP2}(k \leftrightarrow l)$ comprises all paths to which both k and l contribute and $K_{AB}^{PSP2}(k \leftrightarrow l \leftrightarrow m)$ comprises all paths to which k, l and m contribute, etc.

The J-**OC**-PSP2 orbital contributions cannot be determined by setting individual orbitals passive. Instead, the orbitals under consideration must be excluded completely from the CP-DFT procedure, i.e. they have to be *frozen*. This implies that the operator $h^{(N)}$ is modified according to Eqns (6a) and (6b), i.e.

$$h_{ak}^{(N),\mathrm{froz}} = \sum_{a'k'} (\delta_{aa'}\delta_{kk'} - P_{ak,a'k'}^{\mathrm{froz}}) h_{ak}^{(N)} \tag{7a}$$

with

$$P_{ak,a'k'}^{\mathrm{froz}} = \begin{cases} 1 \text{ for } a = a', k = k', k \text{ frozen} \\ 0 \text{ otherwise} \end{cases} \tag{7b}$$

In addition, the passive contributions, i.e. steric exchange and resonance interactions from the frozen orbitals, have to be suppressed, which requires the following replacements in Eqn (4):

$$(\tilde{F}_l^{(B)})_{ak} \rightarrow \sum_{a'k'} (\delta_{aa'}\delta_{kk'} - P_{ak,a'k'}^{\mathrm{froz}})(\tilde{F}_l^{(B)})_{a'k'} \tag{8a}$$

$$F_{kl}^{(0)} C_{al}^{(B)} \rightarrow \sum_{a'k'} (\delta_{aa'}\delta_{kk'} - P_{ak,a'k'}^{\mathrm{froz}}) F_{k'l}^{(0)} C_{a'l}^{(B)} \tag{8b}$$

The $K_{AB}^{PSP2}(\ldots)$ can be computed as differences in K_{AB} values from a conventional SSCC calculation and one or more SSCC calculations with individual orbitals frozen, as shown in detail in Ref. 43. J-**OC**-PSP2 allows SSCC contributions to be classified according to the number of different orbitals involved, no matter how often and in which order the orbitals occur in the orbital path. This is in line with the intuitive understanding of orbital contributions where one asks for the total contribution of a given orbital or set of orbitals rather than an individual orbital path.

Equations (2) and (4) do not determine the full $|\psi_k^{(B)}\rangle$ but only their projection on to the first-order virtual space. In fact, the projection of the $|\psi_k^{(B)}\rangle$ on to the zeroth-order occupied space is not determined. Any set of coefficients $C_{kl}^{(B)}$ that maintains the orthogonality of the $|\psi_k\rangle$ is permissible, i.e. in addition to the excitations described by $C_{ak}^{(B)}$, the orbitals may be subjected to an arbitrary infinitesimal rotation in the zeroth-order occupied space. This arbitrariness simply reflects the fact that the DFT energy and other observable quantities such as the SSCCs are invariant with respect to rotations between the occupied orbitals. Although the total SSCCs are invariant with respect to this ambiguity, an improper choice of the coefficients $C_{kl}^{(B)}$ will lead to artifacts in the individual orbital contributions. In CP-DFT calculations, usually $C_{kl}^{(B)} = 0$ is chosen. This is not only straightforward technically but also natural from the chemical point of view: the response to a perturbation should contain real changes of the orbitals rather than rotations of the occupied orbitals among each other.

Spin–spin coupling and orbital delocalization

The J-**OC**-PSP approaches address the question how *different* orbitals interact in transferring spin information from nucleus B to nucleus A. A complementary question is how the transfer of spin information proceeds *within* an orbital, in particular, which role orbital delocalization plays for the spin–spin coupling mechanism. There are various ways to investigate this question. Wilkens *et al*.[65] used the NJC-1 approach[29] with the goal of decomposing the SSCCs on a per-orbital basis into Lewis contributions, i.e. contributions that can be related to the Lewis structure of the molecule and non-Lewis contributions, which are related to delocalization and repolarization effects. According to the resulting NJC-2 approach, orbital contributions to the FC term are determined as follows:[65]

1. A spin-unrestricted FPT calculation with a small finite extra spin at nucleus B is performed for the closed shell molecule in question.
2. The natural bond orbitals (NBOs)[63] and the corresponding NLMOs[63] are determined for α and β orbitals separately.
3. The FC term of the SSCC and its orbital contributions are calculated for a fictitious system where all Lewis NBOs from (2) are exactly doubly occupied and all non-Lewis NBOs are unoccupied. The resulting value of the FC term is considered the Lewis contribution of the real FC term.
4. The remaining part of the FC term is decomposed according to the non-Lewis NBOs involved. This will yield 'delocalization' contributions related to charge redistributions from the bonding NBO k to the antibonding NBO l^* of the molecule ($k \neq l$) (or from a lone pair orbital into a Rydberg orbital located at another nucleus, etc.) and 'repolarization' contributions related to redistributions into the same region of the molecule (e.g. from k to k^* or to a Rydberg NBO at one of the atoms connected by NBO k).

It should be noted that the non-Lewis contributions to the FC term are not directly connected to the non-Lewis parts of the unperturbed electronic structure. Rather, the non-Lewis terms indicate that delocalization and repolarization proceed differently for α and β spins.

Eventually, this procedure provides a decomposition of K_{AB}^{FC} according to

$$K_{AB}^{FC} = \sum_k \Delta_k \tag{9a}$$

$$\Delta_k = \Delta_k^{(L)} + \Delta_k^{(NL)} \tag{9b}$$

$$\Delta_k^{(NL)} = \Delta_k^{(deloc)} + \Delta_k^{(repol)} \tag{9c}$$

$$\Delta_k^{(deloc)} = \sum_{l^*} \Delta_{k\to l^*}^{(deloc)} \tag{9d}$$

$$\Delta_k^{(repol)} = \sum_{k^*} \Delta_{k\to k^*}^{(repol)} \tag{9e}$$

The NJC-2 contributions to K_{AB}^{FC} are denoted by Δ in line with Ref. 65; the index AB was omitted for brevity in addition to the superscript FC. L and NL stand for Lewis and non-Lewis structure, respectively.

An orbital decomposition along these lines is asymmetric with respect to A and B. Therefore, symmetry is enforced by redoing all calculations with A as perturbing and B as responding nucleus and averaging all results for the two calculations.

The NJC-2 method[65] has a number of serious shortcomings:

1. NJC-2 is available for the FC term only.
2. NJC-2 uses FPT to determine the first-order MOs. As was discussed in the previous sub-section, the first-order MOs and, consequently, the orbital contributions to the SSCCs are not defined unambiguously. CP-DFT allows us to handle this ambiguity in a controlled way, which is not the case for FPT: the unperturbed and perturbed orbitals are calculated independently of each other, including two independent localization procedures. The criterion for the choice of the first-order orbitals in NJC-2 is that the perturbed orbitals should be NLMOs. The generation of NLMOs is a complex procedure comprising several intermediate steps. Hence it is hardly possible to state explicitly how the coefficients $C_{kl}^{(B)}$ are chosen in the NJC-2 procedure. Consequently, one has to expect that the Δ_k contain artificial contributions related to orbital rotations among the occupied orbitals. Clearly, the same restriction applies to NJC-1[29] when it is based on FPT.
3. The NLMOs used in NJC-2 are derived from the NBOs by a symmetric orthogonalization procedure.[63] This implies that, e.g., a core NLMO may have orthogonalization tails from a bond or Rydberg orbital at a different nucleus and that consequently the Δ_k contributions can contain non-physical contributions due to these orthogonalization tails.
4. The Lewis and non-Lewis contributions to the FC term are determined from the perturbed wavefunction. It is not certain that there is a one-to-one correspondence between Lewis and non-Lewis portions in the unperturbed wavefunction and the response of the wavefunction to the perturbation. It would be better to determine the Lewis part of the FC term based on the unperturbed Lewis structure.

With these limitations in mind, we developed a modified approach to determine the Lewis and non-Lewis contributions to the SSCC that is based on the unperturbed Lewis structure and employs a CP-DFT procedure to determine the Lewis part of the SSCC. We start by determining the NBOs for the unperturbed system. Then, the electron structure of the unperturbed system is modified in such a way that all Lewis NBOs are doubly occupied. For the resulting structure, a CP-DFT calculation of the SSCCs is performed. In this calculation, special care is required as the zeroth-order state used is not the actual ground state and the perturbation must be prevented from driving delocalizations into the non-Lewis parts of the real ground state. The CP-DFT calculations are carried out in such a way that the zeroth-order KS operator is chosen as

$$F_{kl}^{(0),NBO} = \sum_m C_{km}^{(0),NBO} C_{lm}^{(0),NBO} \varepsilon_m \tag{10a}$$

$$F_{aa'}^{(0),NBO} = \sum_{a''} C_{aa''}^{(0),NBO} C_{a'a''}^{(0),NBO} \varepsilon_{a''} \tag{10b}$$

$$F_{ak}^{(0),NBO} = 0 \tag{10c}$$

where $C^{(0),NBO}$ is the transformation matrix between the zeroth-order canonical MOs and the NBOs. Note that the virtual NBOs are non-canonical, hence the KS matrix becomes non-diagonal in both the occupied and the virtual space, so that the working equations for the SSCC calculations are slightly different from Eqn (1). The matrix elements of $h^{(B)}$ and $\tilde{F}^{(B)}$ are calculated in the same way as for a conventional CP-DFT calculation.

This procedure provides values for all Ramsey terms, which will be denoted $K_{AB}^{(X,NBO)}$. The $K_{AB}^{(X,NBO)}$ can reasonably be regarded as the Lewis contributions to the SSCC. By taking the difference to the SSCC from a conventional CP-DFT calculation, the non-Lewis term $K_{AB}^{(NL)}$ is obtained. An

orbital analysis of the Lewis and non-Lewis terms can then be performed with the J-**OC**-PSP1 or J-**OC**-PSP2 algorithm.

Visualization of Ramsey and orbital contributions within J-OC-PSP

In addition to decomposing the four Ramsey terms of the SSCC into orbital contributions, we can analyze the spin–spin coupling mechanism by displaying spin polarization density and orbital current density distributions that carry the spin information from the perturbing to the responding nucleus. In this way, the Ramsey terms and their orbital contributions are related to local quantities, which is an important analytical tool within the J-**OC**-PSP approach.[42–47,69]

For the FC term of the SSCC, one can write

$$K_{\mathrm{AB}}^{\mathrm{FC}} = \frac{16\pi}{9}\alpha^2 m^{(B),\mathrm{FC}}(\mathbf{R}_A) \tag{11a}$$

where $m^{(B),\mathrm{FC}}(\mathbf{r})$ is the *FC spin density distribution*, i.e. the spin density generated in the electron system by the FC perturbation of nucleus B:[42]

$$m^{(B),\mathrm{FC}}(\mathbf{r}) = 4\sum_{k}^{\mathrm{occ}} \varphi_k^{(0)}(\mathbf{r})\varphi_k^{(B),\mathrm{FC}}(\mathbf{r}) \tag{11b}$$

Equation (11b) is formulated in terms of space orbitals, which is possible because the response of the α orbitals to the perturbation at nucleus B is just opposite to that of the β orbitals. The representation of the non-contact Ramsey terms becomes more complex because (a) these terms are anisotropic and (b) the corresponding perturbation operators are not localized at the responding nucleus. For each of the non-contact terms, one therefore introduces two kinds of local densities, which reflect the two-step mechanism of spin–spin coupling:[44,45]

(a) A *spin (SD) or current (PSO, DSO) density*, reflecting the interaction of the perturbed nucleus with the electron system. These densities are vector quantities and depend on the orientation of the perturbed spin. This spin or current density is specific for the perturbed but independent of the responding nucleus.
(b) An *energy density*, which is the spin or current density weighted with the perturbation operator at the responding nucleus. This density, which is scalar for all three non-contact terms, can be averaged over all orientations of the perturbing nuclear spin, which provides the energy densities for the isotropic Ramsey terms. The energy densities depend on both the perturbing and the responding nucleus.

The FC spin density introduced above corresponds to (a) and the corresponding FC energy density will show just a δ peak at the responding nucleus.

The SD spin density can be represented as[45]

$$\mathbf{m}_i^{(B),\mathrm{SD}}(\mathbf{r}) = \sum_{i'} m_{(ij)}^{(B),\mathrm{SD}}(\mathbf{r})\mathbf{n}_{i'}, \tag{12a}$$

$$m_{(ij)}^{(B),\mathrm{SD}}(\mathbf{r}) = \sum_{k}^{\mathrm{occ}} 2\varphi_k^{(0)}\varphi_{(ij),k}^{(B),\mathrm{SD}} \tag{12b}$$

where index i gives the orientation of the perturbing nuclear spin and index $i'(i, i' = x, y, z)$ denotes the component of the SD-spin density distribution $\mathbf{m}_i^{(B),\mathrm{SD}}$ under consideration; $\mathbf{n}_i'$ is the unit vector in direction i', and $\varphi_{(ij),k}^{(B),\mathrm{SD}}$ is the first-order orbital corresponding to $\varphi_k^{(0)}$ for a perturbation of the form

$$h_{(ij)}^{(B),\mathrm{SD}} = \alpha^2\left(3\frac{x_{B,i}x_{B,j}}{r_B^5} - \frac{1}{r_B^3}\right) \tag{13}$$

using $\mathbf{r}_B = \mathbf{r} - \mathbf{R}_B$. The six quantities $m_{(ij)}^{(B),\mathrm{SD}}(\mathbf{r})$ are called subcomponents of the SD spin density.

The diagonal components of the SD energy density and the isotropic SD energy density distribution are given by

$$\varrho_{ii}^{(AB),\mathrm{SD}}(\mathbf{r}) = \sum_{i'} \varrho_{(ii')}^{(AB),\mathrm{SD}}(\mathbf{r}) \tag{14a}$$

$$\varrho_{(ii')}^{(AB),\mathrm{SD}}(\mathbf{r}) = h_{(ij)}^{(A),\mathrm{SD}} m_{(ij)}^{(B),\mathrm{SD}}(\mathbf{r}) \tag{14b}$$

$$\varrho^{(AB),\mathrm{SD}}(\mathbf{r}) = \frac{1}{3}\sum_{i} \varrho_{ii}^{(AB),\mathrm{SD}}(\mathbf{r}) \tag{14c}$$

From $\varrho^{(AB),\mathrm{SD}}(\mathbf{r})$, the SD term of the reduced SSCC is obtained by integration:

$$K^{(AB),\mathrm{SD}} = \int \mathrm{d}^3 r\, \varrho^{(AB),\mathrm{SD}}(\mathbf{r}) \tag{15}$$

Analogously, the diagonal components $K_{ii}^{(AB),\mathrm{SD}}$ are obtained from the $\varrho_{ii}^{(AB),\mathrm{SD}}(\mathbf{r})$.

The DSO and PSO current densities for the perturbing nucleus spin oriented along i are[44]

$$\mathbf{j}_i^{(B),\mathrm{DSO}}(\mathbf{r}) = -\alpha^2\varrho^{(0)}(\mathbf{r})\left(\mathbf{n}_i \times \frac{\mathbf{r}-\mathbf{R}_B}{|\mathbf{r}-\mathbf{R}_B|^3}\right) \tag{16a}$$

$$\mathbf{j}_i^{(B),\mathrm{PSO}}(\mathbf{r}) = 2\sum_{k}^{\mathrm{occ}}\left[\varphi_{k,i}^{(B),\mathrm{PSO}}(\mathbf{r})\nabla\varphi_k^{(0)}(\mathbf{r}) - \varphi_k^{(0)}(\mathbf{r})\nabla\varphi_{k,i}^{(B),\mathrm{PSO}}(\mathbf{r})\right] \tag{16b}$$

The corresponding energy densities (X = PSO, DSO) are given by[44]

$$\varrho_{ii}^{(AB),X}(\mathbf{r}) = \alpha^2\mathbf{n}_i\left(\mathbf{j}_i^{(B),X}(\mathbf{r}) \times \frac{\mathbf{r}-\mathbf{R}_A}{|\mathbf{r}-\mathbf{R}_A|^3}\right) \tag{17a}$$

$$\varrho^{(AB),X}(\mathbf{r}) = \frac{1}{3}\sum_{i} \varrho_{ii}^{(AB),X}(\mathbf{r}) \tag{17b}$$

In analogy with Eqn (15), $K_{ii}^{(AB),X}$ and $K^{(AB),X}$ follow from the corresponding energy densities by integration.

Computational details

The molecules investigated in this work are shown in Scheme 1. All SSCC calculations were carried out with the CP-DFT method described previously.[22] In the case of the hydrocarbon molecules, the hybrid functional B3LYP[31,70,71] and the basis set (11s,7p,2s/6s,2p)/[7s,6p,2d/4s,2p][72] were used because CP-DFT/B3LYP/[7s,6p,2d/4s,2p] is known to lead to reliable SSCCs $^nJ(^{13}\mathrm{C},^{13}\mathrm{C}) = {}^nJ(\mathrm{C,C})$, $^nJ(^{13}\mathrm{C},^{1}\mathrm{H}) =$

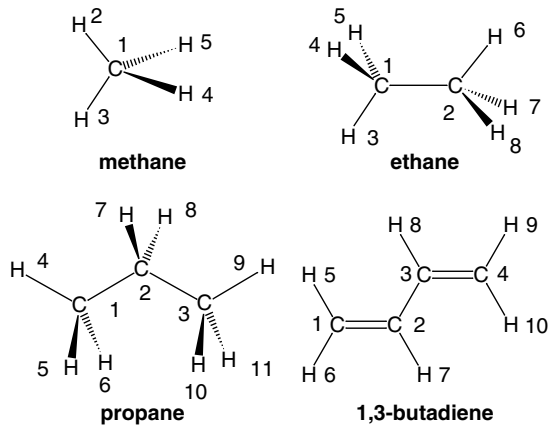

Scheme 1

^nJ(CH), and $^nJ(^1H,^1H) = {}^nJ$(H,H) in the case of hydrocarbons.[22,23]

For CH_4, the experimental geometry[73] was applied whereas for the other molecules shown in Scheme 1, B3LYP/6–31G(d,p) (ethane, propane) or B3LYP/[7s,6p,2d/4s,2p] optimized geometries (1,3-butadiene) were used.

NJC-1 results[29] were obtained by summing J-**OC**-PSP orbital contributions. In the original NJC-1 approach, each orbital contribution is derived as the average of two calculations setting once nucleus A and once nucleus B as the perturbing nucleus:

$$K(\mathrm{NJC})^k_{AB} = \frac{K(\mathrm{NJC})^{k,A}_{AB} + K(\mathrm{NJC})^{k,B}_{AB}}{2} \tag{18}$$

This is necessary because of the nuclear dependence of the term $K^{(k,l)}_{AB}$ in Eqn (18).

Equation (18) can be rewritten as

$$K(\mathrm{NJC})^k_{AB} = K^{\mathrm{PSP1}}_{AB}(k) + \frac{\sum_{l\neq k}^{occ}(K^{\mathrm{PSP1}}_{AB}(k \leftarrow l) + K^{\mathrm{PSP1}}_{BA}(k \leftarrow l))}{2} \tag{19}$$

which in turn can be rewritten as

$$K(\mathrm{NJC})^k_{AB} = K^{\mathrm{PSP1}}_{AB}(k) + \frac{\sum_{l\neq k}^{occ}(K^{\mathrm{PSP1}}_{AB}(k \leftarrow l) + K^{\mathrm{PSP1}}_{AB}(l \leftarrow k))}{2} \tag{20}$$

where all terms on the right-hand side are available from a J-**OC**-PSP1 calculation. Equation (20) reveals that the NJC contribution of occupied orbital k contains both the orbital relaxation term K^k_{AB} and the average steric exchange contribution between orbital k and all other orbitals l. Therefore, one can only obtain a crude idea about the transmission mechanism.

The J-**OC**-PSP analysis[42,43] and the orbital-selected SSCC calculations were carried out for LMOs obtained with a Boys localization[62] where however core, σ and π-orbitals are separately localized for reasons described elsewhere.[42] All discussions are based on LMOs, which also holds when considering π-orbitals in a conjugated system.

All Ramsey densities (see the previous sub-section) and selected orbital contributions to these densities are represented in form of contour line diagrams, where the contour levels are given by a geometric progression with the ratio of $100^{1/5}$ between two subsequent contours. All SSCC calculations and the J-**OC**-PSP analysis were performed with the *ab initio* program package COLOGNE 2003.[74]

RESULTS AND DISCUSSION

In previous work, we demonstrated that J-**OC**-PSP can be applied to all Ramsey terms, not just the FC term.[43–47] Since most of the analytic investigations of the spin–spin coupling mechanism have focused in the past on hydrocarbons and since in these cases the FC term is mostly dominant, we will consider in the following also the FC coupling mechanism. In this connection, we will discuss the appropriate description of the one-bond FC coupling mechanism in hydrocarbons, the controversial explanations for vicinal proton–proton coupling, the coupling via back-lobe interactions in saturated hydrocarbons and the coupling mechanism in conjugated π-systems.

Results obtained for the molecules shown in Scheme 1 are summarized in Tables 1 and 2. We will discuss in the following typical features of the spin–spin coupling mechanism as they are reflected by the J-**OC**-PSP and the NJC methods. In all cases, SSCCs J(A,B) related to reduced SSCCs $K(A,B) = (2\pi/\hbar)J(A,B)/(\gamma_A\gamma_B)$ via the gyromagnetic ratios γ of the coupling nuclei A and B are given in hertz. We simplify the notation by using the terms ^nX(A,B) with

Table 1. Orbital contributions to the NMR spin–spin coupling constant ^1J(C,H) of methane[a]

	J-**OC**-PSP					J-**OC**-PSP					NJC-1	
	LMOs					NLMOs					LMOs: total	NLMOs: total
Term[b]	PSO	FC	SD	DSO	Total	PSO	FC	SD	DSO	Total		
$^1J(bd)$	−0.80	165.16	−0.62	−1.01	162.73	0.40	58.96	−0.61	−1.31	57.45	147.54	91.25
$^1J(ob)$	1.98	−11.11	0.79	1.16	−7.19	0.86	−4.09	0.79	1.53	−0.90	−18.97	−8.04
$^1J(c)$	0.00	−0.09	0.00	0.00	−0.09	0.00	6.00	0.00	−0.07	5.93	−4.50	40.89
$^1J(bd, ob)$	0.25	−22.85	0.05		−22.54	0.16	−8.51	0.05		−8.3		
$^1J(bd, c)$	−0.01	−7.75	0.00		−7.77	−0.77	76.67	−0.01		75.89		
$^1J(ob, c)$	0.01	−1.08	0.00		−1.06	0.77	−6.74	0.00		−5.98		
^1J(C,H)	1.42	122.29	0.22	0.15	124.08	1.42	122.29	0.22	0.15	124.08	124.08	124.08

[a] All values in hertz.

[b] c = core; bd = bond; ob = other bonds.

Table 2. Decomposition of the vicinal spin–spin coupling constant ^{3}FC(H3,H6) of ethane into orbital contributions in dependence of the dihedral angle τ(H3C1C2H6)[a]

τ(H3C1C2H6)	^{3}FC (C1H3) +^{3}FC (C2H6)	^{3}FC (C1H3 ↔ C2H6)	^{3}FC (others)	^{3}FC (total)
*J-**OC**-PSP, LMOs*				
0	5.48	7.18	0.89	13.54
30	4.22	5.38	0.63	10.22
60	1.58	2.09	0.15	3.82
90	0.01	0.56	0.04	0.61
120	1.31	2.51	0.62	4.44
150	4.23	6.20	1.50	11.92
180	5.62	7.91	1.90	15.44
*J-**OC**-PSP, NBOs*				
0	0.72	3.84	0.17	4.73
30	0.51	2.75	0.03	3.29
60	0.12	0.91	−0.21	0.82
90	−0.14	0.26	−0.24	−0.12
120	−0.10	1.32	0.03	1.25
150	0.11	3.01	0.41	3.53
180	0.22	3.76	0.56	4.54

[a] Dihedral angle τ(H3C1C2H6) in degrees, all other values in hertz. For the numbering of atoms, see Scheme 1. The contributions FC(NBO) were obtained using NBOs occupied by exactly two electrons in the J-**OC**-PSP analysis (see text).

X = FC, SD, PSO, DSO rather than ${}^nJ^X_{A,B}$ for the Ramsey terms. In the same way, we will use X(LMO) rather than ${}^nJ^{X,LMO}_{A,B}$ where the identification of the coupling nuclei will be dropped if the latter are automatically identified by the LMO considered.

Comparison of J-OC-PSP and NJC methods: choice of the orbitals

The NJC-2 analysis[65] is tightly connected with the use of NLMOs,[63] whereas J-**OC**-PSP can be performed with any set of LMOs (normally it uses Boys LMOs).[42–50] The total SSCCs and the four Ramsey terms of a given molecule are independent of the choice of the orbitals used in the CP-DFT calculations. This does not apply, however, to the individual orbital contributions. Nevertheless, results obtained with LMOs or NLMOs can reveal which orbitals and in this way which analysis method is more reasonable.

The form of the NLMOs[63] is similar to that of the LMOs obtained by Boys localization.[62] However, owing to the construction of the NLMOs via natural atomic orbitals (NAOs),[63] the NLMO core orbital contains a tail made up from valence shell orbitals. Analogously, the bond and lone pair orbitals become contaminated by the core orbitals. Hybrid orbital calculations of methane employing the NBO analysis[63] demonstrate this. The core NLMO of methane includes a contribution of 1.5% from the valence shell orbital (corresponding to a coefficient of −0.1223 for the a_1-symmetrical MO and of 0.9925 for the carbon core MO). The population of the tail is tiny, but the resulting change of the Ramsey densities and eventually the orbital contributions contains terms linear in the expansion coefficients, i.e., the mixing, may give rise to considerable changes in the SSCC orbital contributions. This is reflected by the J-**OC**-PSP analysis of the SSCCs of methane in terms of Boys LMOs and NLMOs (see Table 1).

In Table 1, the ^1J(C,H) value of methane, its PSO, FC, SD and DSO terms and as the corresponding orbital contributions are listed in terms of both LMOs and NLMOs. NJC-1 orbital contributions calculated as described earlier are also given in Table 1.

The CH bond orbital term $^1J(bd, \mathrm{CH}) = {}^1J(bd)$ always leads to a positive contribution to the total ^1J(C,H) value and its FC term, independent of method and orbitals used. However, $^1J(bd)$ is about three times as large for Boys LMOs as for NLMOs. [J-**OC**-PSP; $^1J(bd)$, LMOs 162.7; NLMOs 57.5 Hz, see Table 1]. The contributions of the other CH bond orbitals [$^1J(ob)$] to the ^1J(C,H) value are negative (J-**OC**-PSP, LMOs −7.2; NLMOs −0.9 Hz), i.e. they play a similar role to the lp orbital for the FC spin–spin coupling mechanism by extending the coupling path by one orbital and reverting in this way the sign of the contribution.

The one-orbital effect of the core electrons must be small due to their strong localization at one nucleus. This, however, does not exclude that non-negligible (but still relatively small) two-orbital contributions involving the core orbitals are found because a bd or lp orbital can reach into the core region and lead there to steric exchange effects. This is verified by the J-**OC**-PSP analysis carried out with LMOs [$J(c)$, −0.1; $J(bd, c)$, −7.8; $J(ob, c)$, −1.1 Hz; Table 1]. However, the J-**OC**-PSP analysis in terms of NLMOs leads to a $J(c)$ of 6 Hz and a suspiciously large $J(bd, c)$ value of 75.9 Hz, which accounts for more than 60% of the total ^1J(C,H) value.

The large one-orbital term $J(c)$ found for the NLMO description can be explained by the orthogonalization tails of the c-NLMO, which provides contacts with the four H nuclei. There are two possible mechanisms that probably contribute to the large $J(bd,c)$ value, both of which are eventually due to the mixing between the c and the bd LMOs in the NLMOs: First, $J(bd)$ contains a considerable portion self-exchange. In the LMO representation, this self-exchange appears in $J(bd)$, whereas the mixing of c and bd orbitals transforms a part of this self-exchange into a steric interaction between c- and bd-NLMOs. Second, in the LMO representation there is no resonance interaction between bd orbitals and c orbital, as the two groups of orbitals are localized separately. For NLMOs, however, the mixing of core and bond orbitals allows for a resonance interaction. Overall, the analysis of the J-**OC**-PSP results for LMOs and NLMOs reveals that the mixing of orbitals occurring in the generation of NLMOs gives rise to a non-physical description of the spin–spin coupling mechanism in terms of individual orbitals. Since the NJC-2 analysis[63] is tightly connected with NLMOs, the data in Table 1 clearly speak against its use. For the purpose of avoiding the observed inconsistencies for NLMOs, one would have to construct the underlying NBOs[63] in a different way rather than by symmetric orthogonalization of a set of non-orthogonal LMOs. One would have to use the Schmidt orthogonalization to keep the core NBOs free from orthogonalization tails. J-**OC**-PSP is not restricted to a particular type of LMOs,

and the non-physical core-valence interactions can easily be avoided by using Boys LMOs and localizing the different subspaces (core, σ valence, π valence) separately.

Analysis of the vicinal proton–proton coupling constants

The vicinal SSCC $^3J(\mathrm{H,H}) = {}^3J(\mathrm{HCCH})$ has been extensively used as stereochemical probe for studying conformational features[75] because of its sensitivity to variations in the associated dihedral angle τ(HCCH). The theoretical basis for the dependence of $^3J^{\mathrm{FC}}(\mathrm{H,H}) = {}^3\mathrm{FC(H,H)}$ on τ was first discussed by Karplus (Karplus relationships).[3,4] Despite the fact that the Karplus relationships have been the subject of many theoretical investigations,[1,3,4,75,76] there are still open questions concerning the transmission mechanism of the SSCC ^{3}FC(H,H) and its dependence on τ. By using a modified sum over states (SOS) approach, Esteban *et al*. argued that the main contribution to ^{3}FC(H,H) of ethane results from a through-space interaction term.[76] Wilkens *et al*.[65] discussed ^{3}FC(H,H) of ethane in terms of their NJC-2 analysis. They suggest that about 70% of the ^{3}FC(H,H) term is due to the Lewis contribution $\Delta^{(\mathrm{L})}$, which implies that a through-bond (H—C—C—H) rather than through-space FC spin–spin coupling mechanism is operative. However, $\Delta^{(\mathrm{L})}$ of NJC-2 is not calculated with the correct zeroth-order Lewis-wavefunction, but a total wavefunction including first-order effects as was pointed out earlier.

In Table 2, the vicinal proton–proton coupling constant ^{3}FC(H3,H6) of ethane (for atom numbering, see Scheme 1) and its leading J-**OC**-PSP1 orbital contributions are listed both for the real structure, described with Boys LMOs, and for the Lewis structure, which is obtained by making all Lewis NBOs exactly doubly occupied and keeping all other NBOs unoccupied. The NBO contributions determine the contributions of the Lewis structure. Since the non-core NLMOs are similar to the corresponding LMOs, one can take the difference between an LMO contribution and the corresponding NBO contribution to obtain a good estimate of FC(NL) resulting from the non-localization density. For the purpose of comparing results with those of the NJC-2 analysis (limited to the FC term),[65] just the FC term is considered, which, however, dominates the SSCC ^3J(H3,H6) of ethane.

In Fig. 1, orbital contributions are plotted as a function of the H3C1C2H6 dihedral angle τ. The J-**OC**-PSP1 analysis reveals that the steric exchange two-orbital contribution $^3\mathrm{FC}[\sigma(\mathrm{C1H3}) \leftrightarrow \sigma(\mathrm{C2H6})]$ and the bond orbital relaxation contributions $^3\mathrm{FC}[\sigma(\mathrm{C1H3})]$ and $^3\mathrm{FC}[\sigma(\mathrm{C2H6})]$ dominate ^{3}FC(H3,H6) (see Table 2) and govern the form of the Karplus relationship between ^{3}FC(H3,H6) and dihedral angle τ (see Figure 1). The sum of these contributions accounts for 86–96% of the total SSCC (Table 2 and Fig. 1). The steric exchange and bond relaxation contributions are always positive for ethane, the steric exchange contribution being slightly larger than the sum of the bond relaxation

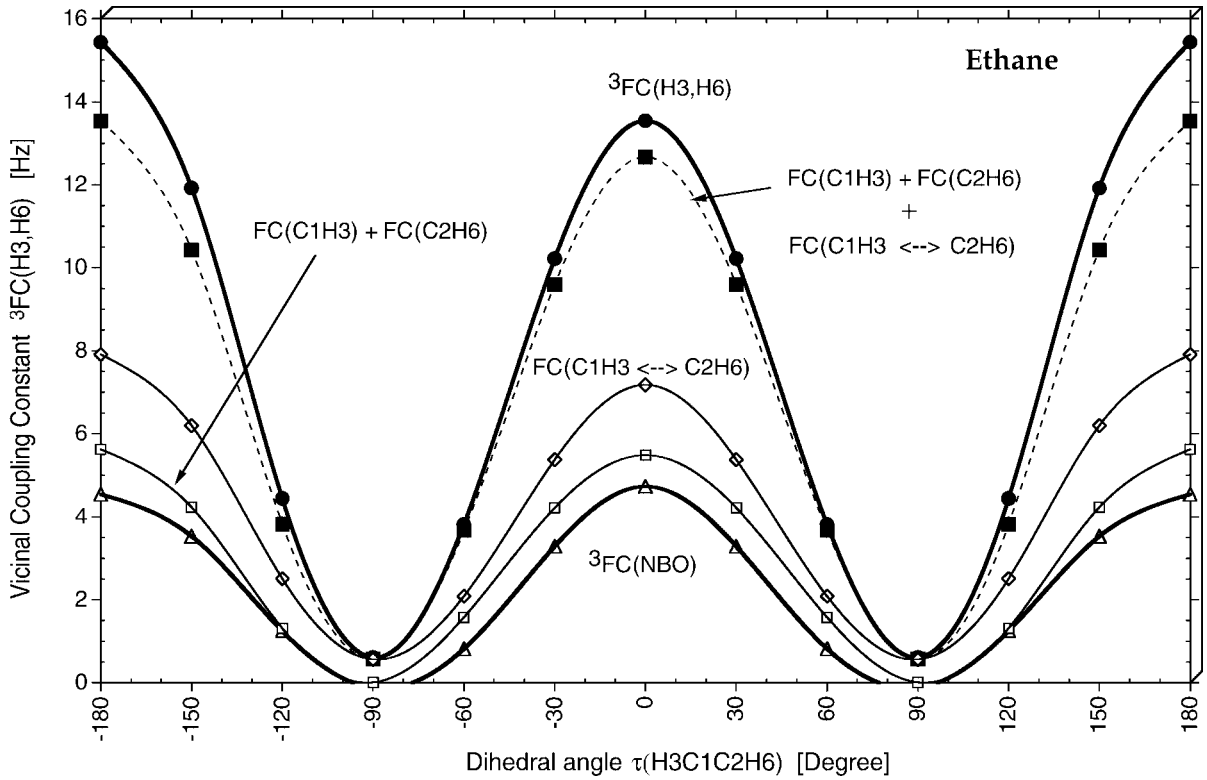

Figure 1. Karplus curve (bold line with filled circles) for the term ^{3}FC(H3,H6) of ethane (rigid rotor model) calculated at the CP-B3LYP/[7s,6p,2d/4s,2p] level of theory. The orbital relaxation terms $^3\mathrm{FC}[\sigma(\mathrm{C1H3})] + {}^3\mathrm{FC}[\sigma(\mathrm{C2H6})]$, the two-orbital steric exchange interaction contribution $^3\mathrm{FC}[\sigma(\mathrm{C1H3}) \leftrightarrow \sigma(\mathrm{C2H6})]$ and the sum of these terms (dashed line with filled squares) are given. Also shown is the Lewis contribution as calculated via the NBO contribution ^{3}FC(NBO) (bold line with open triangles). For the numbering of atoms, see Scheme 1.

MRC

contributions. The bond relaxation terms are strongly influenced by the non-Lewis contribution (zero at $\tau = 90°$, large values at $\tau = 0$ or 180°; Table 2, Fig. 1), less by the Lewis contribution as one can verify by taking the difference between ^{3}FC[σ(CH)] and ^{3}FC^{NBO}[σ(CH)] terms. Contributions from other orbitals are small but non-negligible owing to their small density at the site of either nucleus H3 or H6. These results are consistent with chemical intuition.

Replacing the real by the Lewis structure leads to substantial changes in the FC coupling. As the J-**OC**-PSP1 results in Table 2 show, the sum of ^{3}FC^{NBO}[σ(C1H3)] and ^{3}FC^{NBO}[σ(C2H6)] decreases drastically and becomes even negative in the range $\tau = 90$–120°. The exchange interaction term ^{3}FC^{NBO}[σ(C1H3) $\leftrightarrow$ σ(C2H6)] is decreased to about half (Table 2). The total variation of ^{3}FC in dependence on τ is decreased to about one-third, i.e. a true Lewis determinant cannot reproduce the experimental SSCC of ethane for angles close to 0 and 180° (Table 2) and, therefore, fails to reproduce the Karplus curve even qualitatively (Fig. 1). Effects of the non-Lewis density (comprising delocalization and other non-localization densities) reflected by the difference FC(total) $-$FC^{NBO} are more important than Lewis contributions. In view of these findings, the conclusion of Wilkens *et al*.[65] that ^{3}FC(H3H6) should be dominated by Lewis contributions becomes questionable.

The results of our J-**OC**-PSP1 analysis allow us to locate and quantify the inconsistencies in the NJC-2 approach that eventually lead to the counterintuitively large Lewis contribution to ^{3}FC. For that purpose, we note that the non-Lewis part of an orbital may play three different roles in the FC coupling mechanisms:

1. An orbital whose Lewis part encloses the perturbing nucleus but not the responding one may have a delocalization tail stretching to the responding nucleus, allowing for a direct spin-information transfer through this orbital.
2. An orbital whose Lewis part encloses the responding but not the perturbing nucleus may have a delocalization tail stretching to the perturbing nucleus, again allowing direct transfer of spin information through this orbital.
3. Delocalization tails may allow or enhance the resonance or steric exchange interaction between orbitals, increasing the contribution of two- or more-orbital paths to the spin–spin coupling mechanism.

The results in Table 2 indicate that all three effects play a role for ^{3}FC(H3,H6): the difference between the Boys-LMO and NBO one-orbital terms shows the dominating role of mechanisms (1) and (2) for these terms [note in this connection that the contributions from σ(C1H3) and σ(C2H6) are equal for reasons of symmetry] whereas the two-orbital contribution σ(C1H3) $\leftrightarrow$ σ(C2H6) is influenced by mechanism (3). This is confirmed by the FC spin densities for the J-**OC**-PSP1 contributions shown in Fig. 2 (the perturbation is applied at H6). The FC spin density related to ^{3}FC^{LMO}(C2H6) [Fig. 2(a)] is concentrated around the C2H6 bond but contains a delocalization tail at C1H3, which makes one-orbital FC coupling through σ(C2H6) possible. For the NBO structure [Fig. 2(d)], the spin polarization is less delocalized, resulting in a much smaller spin density at H3 and eventually a weaker one-orbital FC coupling (0.11 Hz as compared with 2.8 Hz for LMOs; Table 2, $\tau = 180°$). Analogously, the delocalization tail of the σ(C1H3) LMO stretching to H6 enables this orbital to receive spin information from the nucleus at H6 and to convey it to H3 [Fig. 2(b)] in distinction to the corresponding NBO [Fig. 2(e)], which obtains only a small spin polarization at H6. The ^{3}FC[σ(C1H3) $\leftrightarrow$ σ(C2H6)] term is dominated by the σ(C1H3) $\leftarrow$ σ(C2H6) contribution. The σ(C1H3) $\leftarrow$ σ(C2H6) FC spin density for the LMOs [Fig. 2(c)] shows the FC spin density induced in σ(C1H3) via σ(C2H6). It is noteworthy that there is a concentric region with β surplus spin density around H6, which indicates the impact of σ(C2H6) on the delocalization tail of σ(C1H3). This concentric region is missing in the corresponding NBO spin density [Fig. 2(f)]. Otherwise, the LMO and NBO two-electron FC spin densities resemble each other, apart from the fact that the former is larger by a factor of ~2. This indicates that the overall interaction between orbitals σ(C2H6) and σ(C1H3) is enhanced by their delocalization tails, which finally results in a stronger FC coupling (7.9 Hz compared with 3.8 Hz for NBOs; Table 2, $\tau = 180°$).

The general conclusion from the J-**OC**-PSP1 analysis is that non-Lewis rather than the Lewis contributions dominate the vicinal SSCC ^{3}FC(H3,H6) in ethane, i.e. a through-space rather than through-bond spin–spin transfer mechanism is preferred for the FC term. The rear lobes and the long delocalization tails carry the spin information and lead to the spin transfer through space rather than through bond, which is confirmed by the fact that the σ(CC) orbital contribution is minimal. Hence the dependence of ^{3}FC(H3,H6) on the dihedral angle τ results from the non-Lewis part of the FC term where less than 50% of the τ dependence is due to the one-orbital and more than 50% to the two-orbital FC contributions involving the CH bond orbitals. If τ decreases from 180 to 90°, the responding (perturbing) nucleus moves out of the tail region of the CH bond orbital at the perturbing (responding) nucleus. At the same time, the through-space steric exchange interaction between the CH bond orbitals decreases to zero so that at 90° the FC term of ^{3}FC(H3,H6) approaches a value close to zero. If ethane continues to rotate, the FC term increases again and obtains another maximum for $\tau = 0°$. In this conformation, the back lobes of the CH bond orbitals can interact in a similar yet slightly weaker way than in the *trans* arrangement, thus leading to an FC term of SSCC ^{3}FC(H3,H6) close to the value calculated for $\tau = 180°$ (see Table 2). This explanation is in line with the early analyses of Karplus[3,4] and Barfield[5], but differs from that obtained with the NJC-2 analysis.[65]

The question remains of why the NJC-2 analysis fails to decompose properly the SSCC ^{3}FC(H3,H6) in ethane and instead suggests a dominance of the Lewis contributions. In NJC-2, the distinction between Lewis and non-Lewis contributions is done merely from the viewpoint of the responding nucleus. In other words, only effect (1) in the list above is regarded as a non-Lewis contribution; (2) and (3) appear as a part of the Lewis contribution. For ^{3}FC(H3,H6), this means

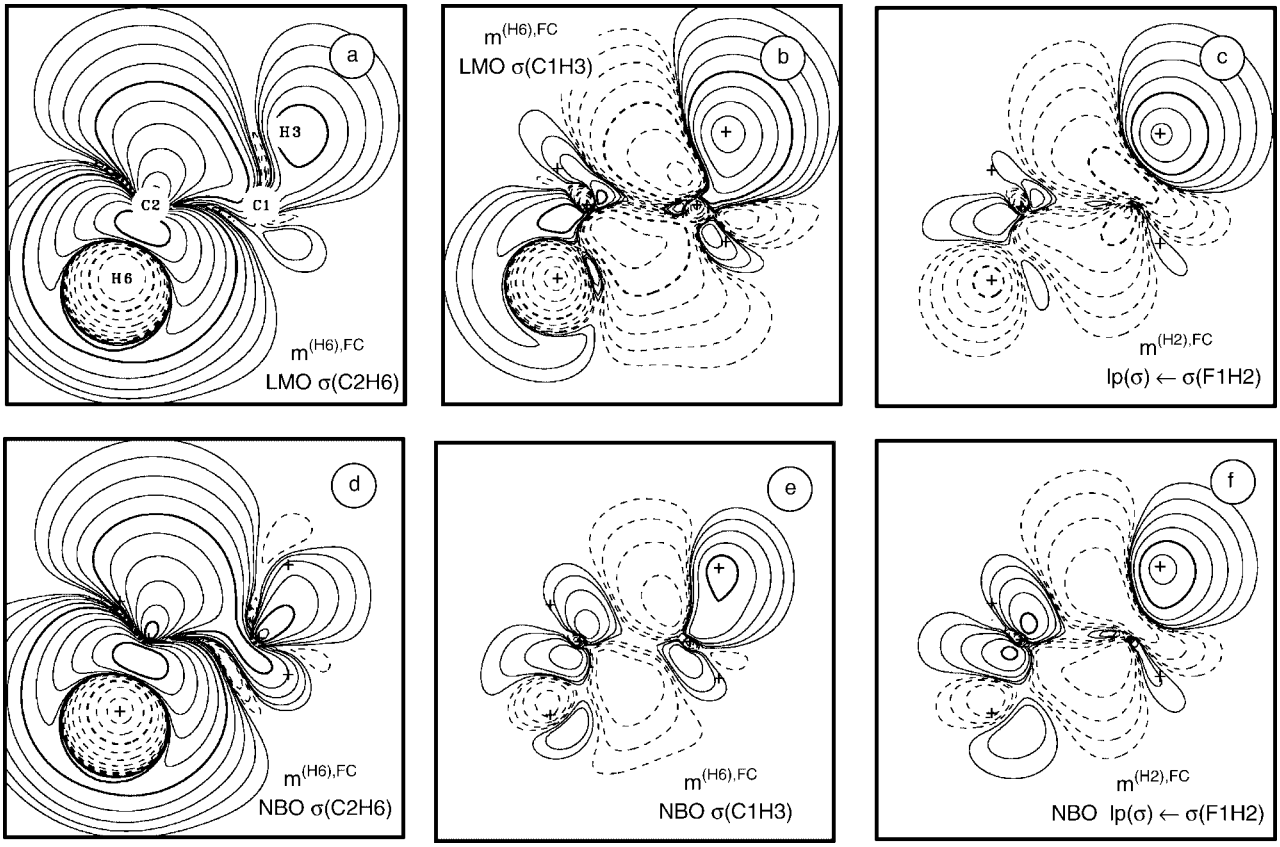

Figure 2. FC spin densities corresponding to the dominant J-**OC**-PSP1 contributions to ^3J(H,H) in ethane for the real electronic structure and the Lewis structure calculated at the CP-DFT/B3LYP/[7s,6p,2d/4s,2p] level of theory. (a) FC spin density distribution for the one-orbital contribution σ(C2H6) in the real structure, scaled by 100. (b) FC spin density distribution for the one-orbital contribution σ(C1H3) in the real structure, scaled by 1000. (c) FC spin density distribution for the two-orbital contribution [σ(C1H3) ← σ(C2H6)] in the real structure, scaled by 1000. (d) FC spin density for the one-orbital contribution σ(C2H6) in the Lewis structure, scaled by 100. (e) FC spin density for the one-orbital contribution σ(C1H3) in the Lewis structure, scaled by 1000. (f) FC spin density for the two-orbital contribution [σ(C1H3) ← σ(C2H6)] in the Lewis structure, scaled by 1000. The contour line diagrams are given for a plane containing H6, C1, C2 and H3. Solid contour lines indicate a dominance of α spin density (positive amplitudes) and dashed contour lines β spin density (negative amplitudes). The spin of the perturbing nucleus H6 is assumed to be α. Contour lines for 0.1 and 10 are printed in bold.

that ^{3}FC[σ(C1H3)] and ^{3}FC[σ(C1H3) ↔ σ(C2H6)] are considered as pure Lewis contributions, and only ^{3}FC[σ(C3H6)] is regarded as having predominantly non-Lewis character. Keeping in mind that ^{3}FC[σ(C1H3)] and ^{3}FC[σ(C3H6)] are equal for reasons of symmetry, one can estimate the NJC-2 results from by adding half of ^{3}FC[σ(C1H3)] + ^{3}FC[σ(C2H6)] to ^{3}FC[σ(C1H3) ↔ σ(C2H6)] [see Eqn (20)], where the Lewis contributions to ^{3}FC[σ(C1H3)] + ^{3}FC[σ(C2H6)] and all contributions from other orbitals have been neglected. This estimation predicts that ^{3}FC(H3,H6) should vary between 0.6 Hz ($\tau = 90°$) and 9.9 Hz ($\tau = 0°$) or 10.7 Hz ($\tau = 180°$), respectively, in good agreement with the $^3\Delta$(H3,H6) values reported in Ref. 65. This confirms that the obscure findings of the NJC-2 approach[65] are due to an inconsistent separation between Lewis and non-Lewis contributions.

Back-lobe interactions leading to long-range coupling constants

The investigation of the vicinal SSCC ^3J(H3,H6) of ethane has demonstrated that the most important spin–spin coupling mechanism is due to through-space steric-exchange interactions between the rear lobes of the σ(CH) orbitals at the perturbing and responding nuclei. The expected orbital path σ(C2H6) → σ(C1C2) → σ(C1H3) does not provide an important contribution to the coupling mechanism. Utilizing J-**OC**-PSP2, the active and passive σ(C1C2) contributions are calculated to vary in the range −0.1 to −0.7 Hz and 0.3 to 0.5 Hz, respectively so that their total impact on the FC part of the vicinal SSCC ^3J(H3,H6) is between −0.3 and 1 Hz. The idea that the spin information is transported along the bond path has thus to be questioned, and the ^3J(H,H) in ethane could be classified more suitably as a 'through-space SSCC ^2J(H,H)'.

For SSCC over more than three bonds, the coupling along the bond path is even smaller than for the SSCC ^3J(H,H) in ethane. A sizable spin–spin coupling predominantly carried by the FC mechanism requires thus an effective through-space coupling mechanism from the perturbed to the responding nucleus. A prototype for the through-space coupling in saturated hydrocarbons is the 'zig-zag mechanism' that was investigated intensely by Barfield

and co-workers.[8,10] In the C_{2v}-symmetrical equilibrium conformation of propane (see Scheme 1 for numbering of atoms), the four-bond SSCC ^4J(H4–C1–C2–C3–H9) = ^4J(H4,H9) can be considered to follow a zig-zag bond path forming a 'W', i.e. one of the terminal hydrogen atoms at each side is in trans position to the C—C—C skeleton. The W-mechanism of FC spin–spin coupling suggests that effective through-space coupling is possible between the back lobes of the σ(CH) orbitals of these two hydrogen atoms. In Fig. 3, the calculated FC terms and total SSCC ^nJ(H,H) for propane (perturbation at H9) are shown. A comparison of the total J values and their FC contributions shows that spin–spin coupling is dominated by the FC mechanism. Among the SSCCs ^4J(H,H), only that supported by the W-mechanism is sizable (2.6 Hz, see Fig. 3), whereas the other two are smaller than 0.3 Hz. Measured ^4J(H,H) values for molecules with a 'frozen' W-coupling path (e.g. bicyclic molecules) are about 3 Hz, because of the CH_3 rotations in propane, the SSCC ^4J(H,H) for the two in-plane protons seems not be measured, however it has been calculated many times;[8–10] suitable reference values are provided by the propanic SSCCs ^4J(H,H) in norbornanes, which are 3–4 Hz,[77] whereas in propane a smaller value is found owing to the rotational averaging of the three different SSCC ^4J(H,H).

The vicinal SSCC ^3J(H,H) follow the same pattern as observed in the case of ethane: for H—C—C—H adopting a *trans* conformation, the SSCC is 14 Hz, whereas it is 3.2 and 3.8 Hz, respectively, for H—C—C—H in a *gauche* conformation. The geminal SSCCs ^2J(H,H) are between 11.0 and 11.2 Hz.

The J-**OC**-PSP2 analysis makes it possible to separate the through-bond and through-space contributions to the spin–spin coupling mechanism. For this purpose, we performed an SSCC calculation where the σ(CC) bond orbitals and also the σ(CH) orbitals at the central C atom were frozen. Under these conditions, any through-bond coupling along the C—C—C path is suppressed. The resulting FC term of the SSCC ^4J(H4,H9) differs from the original one by less than 0.3 Hz, i.e., more than 90% of the FC coupling mechanism is provided by through-space rather than through-bond coupling. This confirms that FC spin–spin coupling takes place predominantly by the W mechanism suggested by Barfield and co-workers.[8,10] The changes for the other SSCCs ^4J(H,H) are of the same order of magnitude as for SSCC ^4J(H4,H9), the changes being between 0.1 and 0.4 Hz. The vicinal SSCCs ^{3}FC(H,H) are reduced to about one-quarter in the frozen-orbital calculation. In view of the results for ethane, the remaining FC coupling of the vicinal SSCCs has to be ascribed to the one-orbital σ(CH) contribution at the perturbed nucleus [since the σ(CH) orbitals at the responding nucleus are frozen, the second one-orbital σ(CH) and the two-orbital contribution are zero]. The Ramsey terms ^{2}FC(H,H) are decreased by about 0.5 Hz or 5% by freezing the adjoint orbitals, which is due to the fact that the other bond orbital contributions are positive in the case of the geminal SSCC.

In the following we will show that indirect spin–spin coupling through the σ-framework of a molecule can be enhanced by a π mechanism of spin–spin coupling and that

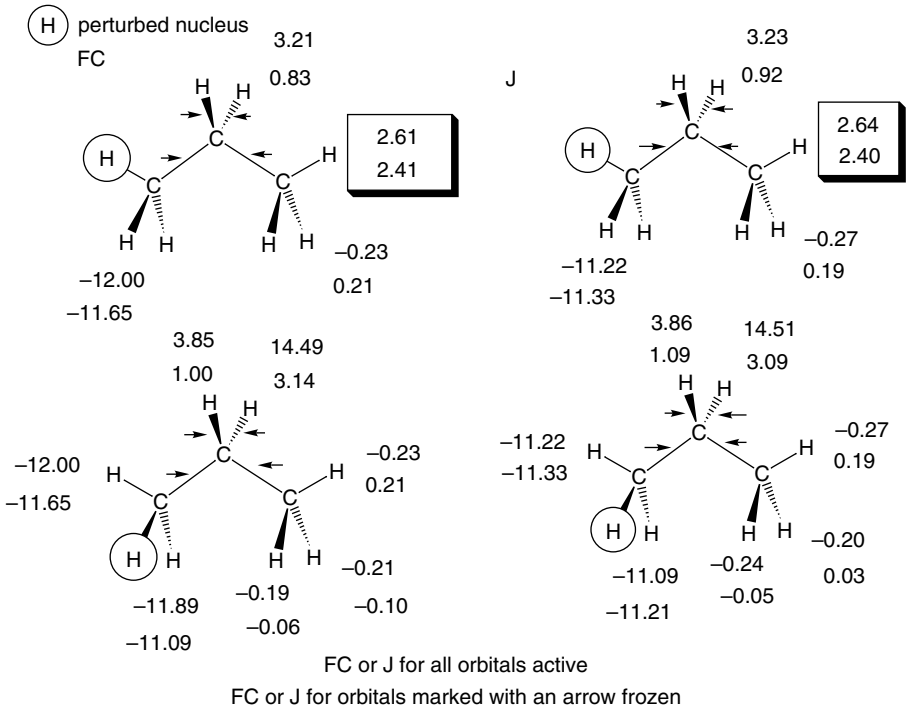

Figure 3. J-**OC**-PSP2 analysis for FC (left) and total proton, proton SSCCs (right) in propane as calculated at the CP-DFT/B3LYP/[7s,6p,2d/4s,2p]//B3LYP/6–31G(d,p) level of theory. Values in normal type are obtained when all LMOs are active; values in italics are obtained when the bond LMOs indicated by small arrows are frozen. The ^{4}FC(H,H) and the ^4J(H,H) values associated with the zig-zag mechanism are enclosed by a box. The encircled H is for all calculations the perturbing nucleus. All values are given in hertz.

in this case through-space interactions also play an important role.

Long-range coupling in π-systems

The discussion in the previous two sub-sections has shown that long-range and even vicinal FC spin–spin coupling is usually based on a through-space rather than just a through-bond coupling mechanism. In the case of ethane, the two-orbital steric exchange interactions between the vicinal CH bd orbitals take place through-space bridging the CC bond. Similarly, the one-orbital contributions of the CH bd orbitals are based on a tail interaction with the responding (perturbing) nucleus, which does not follow the bond path [compare with Fig. 2(a)–(c)]. Hence one could describe the FC spin–spin coupling in these cases as 'through-tail coupling', which expresses the through-space coupling mechanism.

The through-tail FC coupling mechanism explains immediately the influence of electronegative (electropositive) substituents on, e.g., vicinal proton–proton coupling. An electron-withdrawing substituent at a C_3-CH_2 or C_2-CH_2 unit leads to a contraction of the CH bond orbitals and by this also to a contraction of their tails. The one-orbital FC contributions to ^{3}FC(H,H) are decreased where the decrease should be proportional to the electronegativity of the substituent. An electropositive substituent should have an opposite effect, which is confirmed by experimental studies.[78]

Polyenes are known to have sizable long-range SSCCs for five and even more bonds.[8] Also, it has been known for a long time[8,27,66,67] that the π-electron system plays an important role in the long-range spin-information transfer, whereas the through-bond σ-coupling mechanism is important only for short-range SSCCs. There is actually also some through-space σ-coupling via the tail interactions, which is enhanced by the more favorable 120° angles in the polyenes. However, this interaction is known to lead to FC contributions of 0.2–0.3 Hz in the case of five- or six-bond proton–proton SSCCs and quickly decreases to marginal values for larger n.[69] Hence the π-mechanism dominates long-range FC coupling as we were recently able to verify by calculating the π-orbital contributions with the help of J-**OC**-PSP2 for long-range SSCCs ^nJ(H,H), ^nJ(C,H) and ^nJ(C,C) in polyenes.[69]

The π-contribution to long-range FC coupling in polyenes, although important, results from a passive role of the π orbitals in the spin-transfer mechanism: if one of the terminal protons in a polyene is perturbed (α-spin assumed), the density of the corresponding C—H bond will be spin-polarized so that at the C atom α-electron spin dominates. Optimization of exchange interactions in the valence sphere of this C atom will lead to a spin polarization of the pπ electron and by this also of the π-electron pair. The spin information can travel through the π-system from one end of the carbon framework to the other end, spin-polarize there the σ-electrons of the in-plane C—H bonds and thus lead to FC spin–spin coupling between the terminal protons. Since the polarizability of the π-electrons is larger than that of the σ-electrons, the π-mechanism is more effective although the π-orbitals contribute just in a passive rather than active way.

In Fig. 4, the calculated SSCCs ^5J(H,H) of 1,3-butadiene are given together with their total FC and the passive FC(π) contributions. These data (see also Ref. 69) lead to the following conclusions:

1. Long-range SSCCs ^nJ in polyenes are dominated by the FC term, which in turn is dominated with increasing n by the π contributions. The latter decays much more slowly with n than the σ contributions, in spite of the fact that the π system is formally interrupted by C—C single bonds.
2. The π mechanism bridges the formal single bonds in the polyenes without intervention of the σ orbitals in these bonds.

Conclusion (2) can be verified with the data presented in Fig. 4. For butadiene, for instance, the π contribution to SSCC ^{3}FC(C,C) (7.5 Hz, Fig. 4) changes by just 0.03 Hz

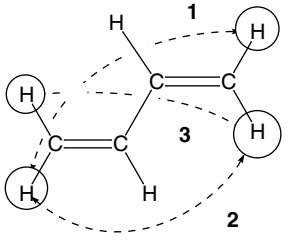

^{5}J(HH) [Hz]

	FC	FC(π)	J	J(exp)
1	1.3	1.0	1.5	1.3
2	0.8	0.9	0.7	0.6
3	0.8	0.9	1.0	0.7

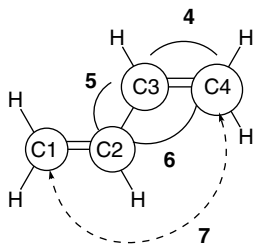

FC(CC) [Hz]

	FC	FC[σ(C2C3)]	FC(π)	FC[σ(C2C3) ↔ π]
4	80.0	–16.4	4.9	1.8
5	56.5	95.5	3.5	3.4
6	1.0	1.0	–2.4	–1.7
7	7.5	0.8	1.9	0.0

Figure 4. J-**OC**-PSP2 analysis for SSCCs ^{4}J(H,H) (top) and ^{n}J(C,C)($n = 1, 2, 3$) (bottom) for 1,3-butadiene as calculated at the CP-DFT/B3LYP/[7s,6p,2d/4s,2p]//B3LYP/[7s,6p,2d/4s,2p] level of theory. Shown are ^{4}FC(H,H), ^{4}FC(π) (top), FC[σ(C2C3)], the total FC(π) and the two-orbital contribution FC[σ(C2C3) $\leftrightarrow \pi$] (bottom) where all values are in hertz. The coupling nuclei are indicated in the structures given on the left by circles. The SSCCs are identified by double-headed arrows and bold numbers.

MRC

if the central σ(CC) orbital is frozen, i.e. the FC coupling mechanism bridges the formal single bond C2—C3 without the necessity to change from the π- into the σ- and back to the π-space. The question arises of how spin information is transferred through the formal single bonds interrupting the π system: are one- or two- and more-orbital contributions dominating? For two- and more-orbital contributions, how is the spin information transported between the orbitals?

For butadiene, the π contribution to ^{3}FC(C,C) is transferred by about 30% by one-orbital terms and about 70% by two-orbital terms.[69] That is, direct transfer through one-orbital terms covers only a minor part of the π FC coupling mechanism. One should expect that two- and more-orbital terms will become even more dominant for couplings bridging more than one formal single bond.

The one-orbital coupling is accomplished by the delocalization tails of the π orbitals. Figure 5(a) and (b) show contour line diagrams of the zeroth-order π(C1C2) and π(C3C4) LMOs of butadiene at a height of 0.6 Å over the molecular plane. They clearly indicate the delocalization tails, which result from excitations π(C1C2) $\rightarrow$ π^*(C3C4) and π(C3C4) $\rightarrow$ π^*(C1C2). The contribution of this orbital to the FC spin density for a perturbation at C1 [Fig. 5(c)] shows an α spin surplus at C4, which is clearly related to the delocalization tail of π(C1C2). For the π(C3C4) orbital [Fig. 5(d)], the delocalization tail at C1 allows an interaction between the perturbing nucleus and the orbital, again resulting in an α spin surplus at C4. This mechanism resembles the one-orbital mechanism for the vicinal HH coupling in ethane.

Analogously, the two-orbital interactions are driven by the delocalization tails of the π(CC) orbitals along the bond axis. Figure 5(c) and (d) reveal that the spin density for the two orbitals agrees around C1 and around C4. Regions with equal sign of the surplus spin result in a positive feedback between orbitals, i.e. an amplification of the spin–spin coupling mechanism. It is therefore the delocalization tail at the next nearest C atom in the chain [C4 for π(C1C2), C1 for π(C3C4)] that allows for the positive feedback between neighboring π(CC) orbitals and thus for the multi-orbital π coupling. In contrast, the sign of the spin densities in the region of the single bond is opposite for the two π(CC) orbitals. This fact counteracts the two-orbital interaction, as has been shown in more detail in previously.[43] Actually, the spin polarized regions of the two π orbitals around the C2—C3 bond avoid each other so as to minimize this counteraction: the spin polarization nearly vanishes around C3 for π(C1C2) and around C2 for π(C3C4).

Overall, the coupling mechanism within the π system is largely analogous to that for the vicinal coupling constants

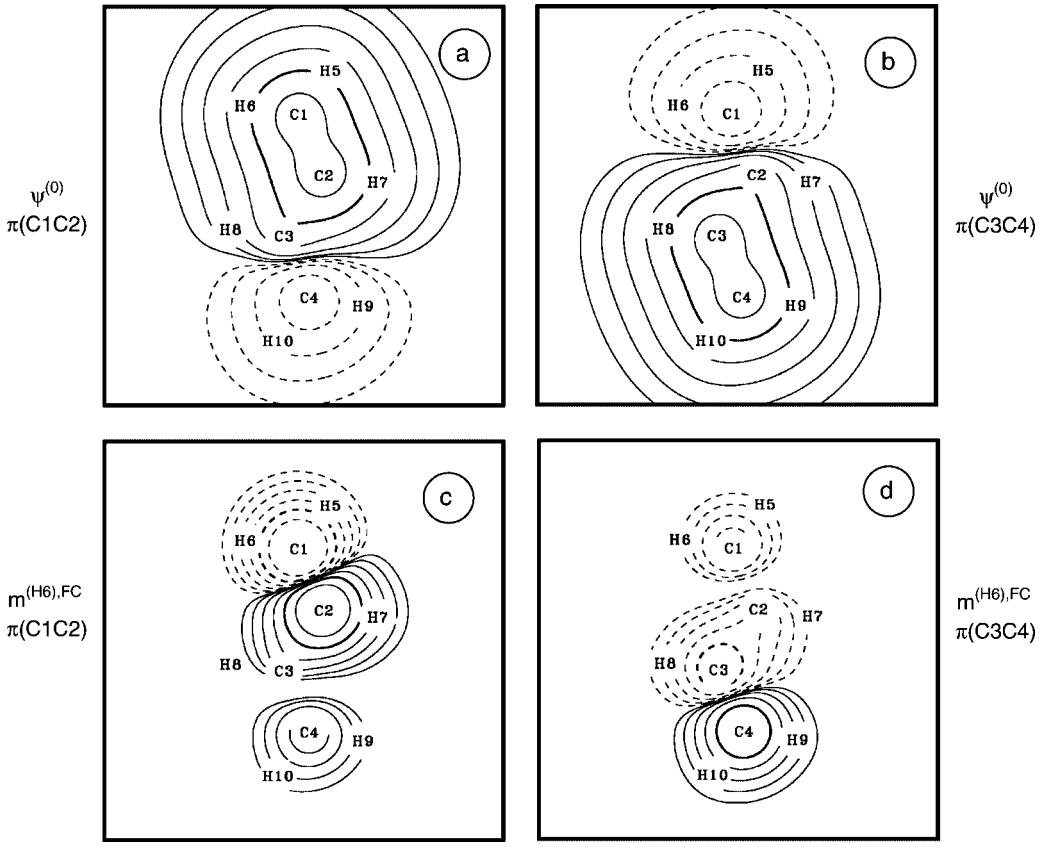

Figure 5. Analysis of the passive π orbital contributions to ^{3}FC(C,C) in 1,3-butadiene as calculated at the CP-DFT/B3LYP/[7s,6p,2d/4s,2p]//B3LYP/6–31G(d,p) level of theory. (a) Zeroth-order LMO π(*C1C2*). (b) Zeroth-order LMO π(*C3C4*). (c) FC spin density distribution for LMO π(*C1C2*). (d) FC spin density distribution for LMO π(*C3C4*). The contour line diagrams are given in a plane 0.6 Å above the molecular plane. Solid contour lines indicate a dominance of α spin density (positive amplitudes) and dashed contour lines β spin density (negative amplitudes). The spin of the perturbing nucleus C1 is assumed to be α. Contour lines for 0.1 and 10 are printed in bold.

in ethane, that is, there is a 'through-tail' coupling, which can be considered as through-space coupling although it is following the bond path (but not the maximum electron density path, which is in the nodal plane of the π-orbitals). We conclude that for long-range coupling in both alkanes and polyenes, the through-space FC mechanism using the delocalization tails of the orbitals is most important for a significant SSCC.

In Fig. 4, the passive FC(π) contributions of some other ^{n}J(C,C) coupling constants are given. Clearly, this is largest for coupling across a double bond (4.9 Hz, SSCC 5; Fig. 4), but still substantial for the coupling across the formal single bond (3.5 Hz, SSCC 6; Fig. 4) and decreases to 1.9 Hz for the FC term of the vicinal SSCC ^{3}J(C,C). As can be seen from the FC(π) values listed in Fig. 4, their sign follows strictly the Dirac vector model (one-bond, +; two-bond, −; three-bond, +; etc.). The $\sigma(C2C3)$ orbital contribution is negative for SSCC 5 because C2C3 represents an external contribution, which is mostly negative;[42] it is large and positive for SSCC 6 where $\sigma(C2C3)$ carries the FC mechanism in an active way; and it is small and insignificant for SSCCs 7 and 8 (Fig. 4). The two-orbital term FC[$\sigma(C2C3) \leftrightarrow \pi$] is significant for one- and two-bond coupling (2.3, 3.6, −2.1 Hz for FC couplings 5, 6 and 7; Fig. 4), but becomes insignificant for the vicinal SSCC ^{3}J(C,C) as discussed above.

STRATEGIES TO DECRYPT THE SPIN–SPIN COUPLING MECHANISM

The current work (seen in connection with previous investigations[42–45]) provides a basis to formulate those criteria that should be fulfilled by any method used to analyze the spin-spin coupling mechanism:

1. It must be applicable to all four Ramsey terms and consequently also to the total SSCC.
2. It must be able to monitor all steps of the spin–spin coupling mechanism from the perturbing to the responding nucleus.
3. As a consequence of (2), it must be capable of providing one-, two- and *m*-orbital contributions where each of these terms is connected with a well-defined physical effect. For example, the one-orbital contributions describe the Ramsey distortion of the orbitals (i.e. the orbital relaxation upon a specific Ramsey perturbation), the two-orbital effects steric exchange interactions, the *m*-orbital effects spin transport, etc.
4. The orbital contributions determined must fulfill the criterion of nuclear independence, i.e. the same orbital contributions are obtained irrespective of the choice of perturbing and responding nucleus, i.e. the direction of the spin–spin coupling mechanism.
5. The orbital contributions should be based on the analysis of zeroth- and first-order orbitals rather than just the total perturbed orbitals. In this connection, the ambiguities in choosing the first-order orbitals must be treated in a well-defined way.
6. It is advisable to distinguish between active and passive orbital contributions to the spin–spin coupling mechanism where the latter lead to three- and *m*-orbital contributions.
7. The method in question should not depend on the type of orbitals used. In this way, it becomes possible to eliminate non-physical orbital contributions, e.g. those of the core orbitals by using appropriate localization techniques.
8. The individual orbital contributions obtained in the analysis should add up to the total SSCC or its Ramsey terms.
9. For the anisotropic Ramsey terms (PSO, DSO and SD), it should be possible to perform the analysis for either the isotropic average of the terms or its Cartesian components.
10. A pictorial description of the orbital terms in a way that the spin–spin coupling mechanism can be followed stepwise is desired.

This work has demonstrated that the J-**OC**-PSP analysis method (comprising levels J-**OC**-PSP1 and J-**OC**-PSP2) combined with a visualization of the individual contributions to the SSCC (Ramsey terms, orbital contributions, Lewis and non-Lewis contributions) in form of spin density and energy density distribution diagrams fulfills all requirements for a detailed analysis of the spin-spin coupling mechanism.

The compliance of J-**OC**-PSP with requirements (2), (3), (4), (5) and (6) is closely connected with the use of a parallel-processing rather than a post-processing approach. This in turn allows us to isolate and quantify individual contributions (e.g. passive contributions from the π orbitals) and to employ the analysis of the SSCC data as a hypersensitive antenna for describing the zeroth-order electron density distribution, in which one is primarily interested, along the whole path between perturbing and responding nucleus.

NJC meets several of these requirements (e.g. in the formulation of NJC-1[29] it can be applied to all four Ramsey terms) and has therefore to be considered as an alternative. However, it does not meet all requirements (1)–(9): both NJC-1 and NJC-2 are essentially one-orbital methods, i.e., they do not allow a direct investigation of steric exchange interactions or of passive orbital contributions. Accordingly, requirements (2), (3) and (6) cannot be met. The way in which two-orbital contributions are introduced in NJC-2 ties the approach to a particular kind of orbitals, viz. NBOs/NLMOs, and therefore violates requirement (7). NJC focuses on the spin-information transfer into the responding nucleus and therefore misses important features of the coupling, as became evident earlier for ^{3}J(HH) in ethane. Requirement (4) is met in NJC-2 by an explicit symmetrization of the contributions.

Another important feature of J-**OC**-PSP is that it is based on a CP-DFT rather than an FPT approach, which accounts for the compliance with requirement (5) and facilitates fulfillment of requirement (1). Problems arise in this connection for NJC, which pragmatically has just been implemented for FC coupling.

Already in the early 1980s, Contreras and co-workers[27,66] and independently Fukui and co-workers[67,68] developed methods that describe the passive role of π orbitals for the

FC coupling mechanism in conjugated π-systems. All these investigations use, similarly to J-**OC**-PSP, parallel-processing approaches. Fukui and co-workers[67] modified the Hessian in such a way that the π orbitals effectively are frozen, whereas Contreras and co-workers[27,66] excluded the π orbitals from the perturbation calculation at the atomic-orbital (AO) level. Although both approaches rest on the same basic idea as our J-**OC**-PSP2 method, they are less general and flexible: direct manipulation of the Hessian is only possible for very small basis sets, i.e. typically for semi-empirical methods as used in Ref. 67. Freezing the π AOs as in Refs 27 and 66 avoids this limitation but prevents the investigation of individual π orbitals or σ-π interactions as is possible in J-**OC**-PSP2.[69] More recently, Esteban *et al*.[76] presented an NBO analysis for the FC coupling mechanism based on a parallel-processing approach, which, although reformulated for a restricted HF calculation, can be generalized straightforwardly to DFT. This method gives a proper account of Lewis and non-Lewis contributions to ^3J(H,H) in ethane.[76] It would, however, fail to reproduce the contributions of passive orbitals, as the perturbation calculation in Ref. 76 is done by standard SOS and thus suppresses steric exchange interaction between orbitals.

It should be mentioned that post-processing methods such as the NJC methods are less costly than a parallel-processing method such as J-**OC**-PSP, for which the gain in detailed information has to be paid for by additional computational efforts. The latter can, however, be reduced in several ways: (i) J-**OC**-PSP is based on the CP-DFT method, which is not expensive even for larger molecules; (ii) J-**OC**-PSP can be applied to groups of orbitals rather than individual orbitals, which reduces the number of calculations substantially; (iii) it is possible to apply J-**OC**-PSP in a stepwise manner (first J-**OC**-PSP1, then J-**OC**-PSP2 for three-orbital effects, J-**OC**-PSP2 for four-orbital effects, etc.), so that with increasing cost the amount of information increases. In most cases one is only interested in particular three- and more-orbital contributions and can therefore reduce the number of SSCC calculations to be done, where results from previous J-**OC**-PSP steps may provide further guidance. In this way, one can minimize the cost/efficiency ratio for each problem individually.

For the purpose of demonstrating the application strategy of J-**OC**-PSP, we discuss as an example the analysis of the unusually large SSCC ^2J(C,C) involving the bridgehead carbon atoms of bicyclo[1.1.1]pentane (see Fig. 6; coupling nuclei are indicated by black balls). Because of the proximity of these nuclei, the question arises of whether spin–spin coupling is due to a strong through-space (THS) mechanism complementing the through-bond (THB) mechanism. Such a question can be answered by using J-**OC**-PSP as indicated in Fig. 6.

For ^2J(C,C), the FC coupling mechanism dominates and, therefore, the analysis can concentrate on this Ramsey term. Spin–spin coupling between the bridgehead C atoms can involve all CC and CH bond orbitals (and core orbitals),

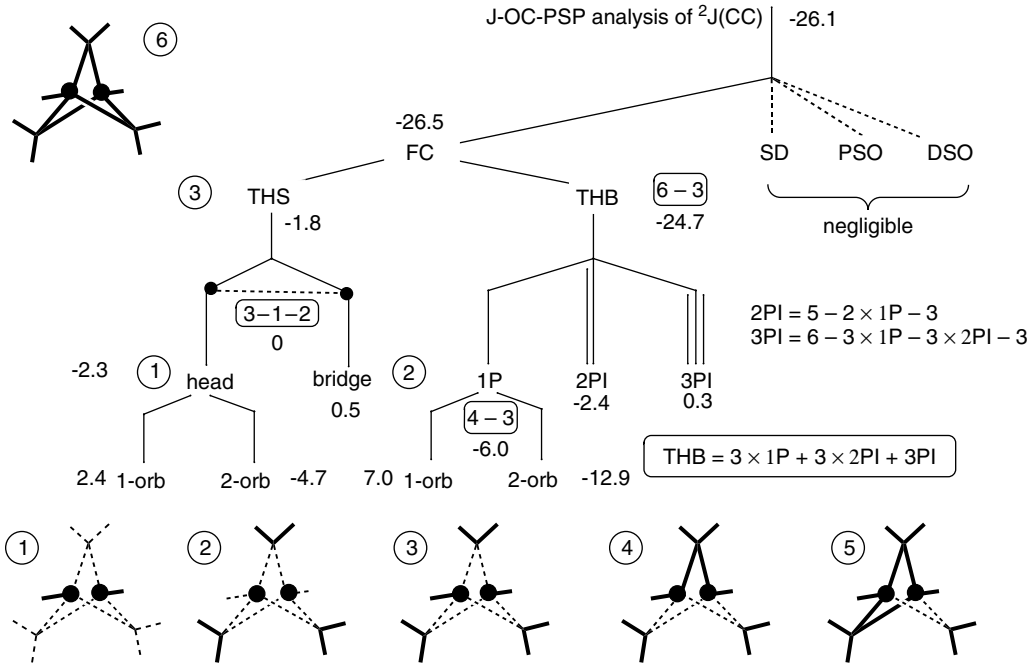

Figure 6. A strategy of analyzing through-space (THS) and through-bond (THB) coupling for the SSCC ^2J(C,C) of bicyclo[1.1.1]pentane with the help of J-**OC**-PSP. In the J-**OC**-PSP2 models **1**–**6** of bicyclo[1.**1**.1]pentane active bond orbitals σ(C — C) and σ(C — H) are given by bold solid lines and frozen bond orbitals by dashed lines. The coupling nuclei are indicated by black balls. The total SSCC is partitioned into contributions presented directly or by differences between the SSCCs ^2J(C,C) obtained for the models shown. The following notation is used: 1-orb and 2-orb, one- and two-orbital contributions; head, contribution of the two headgroup CH bonds; bridge, contribution of the three methylene groups through-space; 1P, contribution of one bridge; 2PI, contribution resulting from bridge–bridge interaction; 3PI, contribution resulting from bridge–bridge–bridge interactions.

which are indicated in the bicyclo[1.1.1]pentane picture **6** (Fig. 6, upper left corner) by bold lines. For the purpose of eliminating the THB coupling paths and thus isolating the THS contributions, the CC bond orbitals are frozen (in calculation **3** in Fig. 6, the frozen bond orbitals are indicated by dashed lines). In this way, a THS contribution of −1.8 Hz is calculated, which is considerably larger than the THS contribution for ^2J(C,C) ≈ ^{2}FC(C,C) in propane, but does not explain the magnitude of the SSCC. From calculations **1** and **2**, one finds that the negative THS term results from the bridgehead CH bonds [calculation **1**, which is reduced by the CH_2 bridge contributions (0.5 Hz)]. The bridgehead CH bond term can be further decomposed into one- and two-orbital terms, which reveals that this term is dominated by the steric exchange interaction between the two bridgehead CH orbitals (−4.7 Hz), which are partly compensated by the corresponding one-orbital Ramsey distortions (2.4 Hz, Fig. 6).

The dominance of the steric exchange term clearly indicates that there is no (weak) bond or bonding interaction between the bridgehead C atoms. Bonding is always indicated by the dominance of the one- over the two-orbital term. In addition, one can calculate the Lewis contributions (see the second section) and determine what role delocalization effects play in the transfer of spin information to and from the bridgehead nuclei. This reveals that the dominating path is via the three bridges.

The contribution of one bridge is calculated to be −6 Hz by combining calculation **4** with calculation **3** (Fig. 6), i.e. the three bridges will contribute −18 Hz if their mutual interaction is not considered. However, the spin polarization of one bridge enhances (decreases) the spin polarization of the other bridges by steric exchange interaction, which causes another negative contribution to ^2J(C,C) (combination of calculations **4**, **5** and **6**; see Fig. 6). This shows that the large magnitude of ^2J(C,C) results from a multipath through-bond coupling mechanism. Further details are obtained when considering the one- and two-orbital terms, i.e. the analysis can be terminated after the first step (just carrying out two calculations) or continued through two more levels to obtain more details.[79]

The J-**OC**-PSP approach is capable of providing a large amount of information on the spin–spin coupling process and can therefore can answer specific questions in this connection. The analysis of the spin–spin coupling mechanism can be complemented by a graphical representation of the Ramsey spin (for DSO and PSO: Ramsey current) and Ramsey energy densities for the total SSCC in addition to the individual J-**OC**-PSP contributions.

The idea of visualizing magnetic properties in terms of a density was first presented by Jameson and Buckingham.[80] Recently, a number of approaches for the visualization of the spin-spin coupling mechanism have been suggested. Malkina and Malkin[81] developed a local analysis of the FC coupling on the basis of a mixed second-order FPT. In this approach, both a spin density and an energy density are introduced for the FC term. Their definition of the densities in[81] is basically different from that in J-**OC**-PSP, which fully rests on first-order perturbed orbitals. Soncini and Lazzeretti[82] introduce a Ramsey energy density that is similar to the J-**OC**-PSP Ramsey energy densities. In contrast to J-**OC**-PSP, the energy densities for the FC and SD terms are defined[82] using a spin current density rather than the spin density itself. This allows one to define a reasonable energy density for all four terms including the FC term. However, one has to abandon the physically transparent picture that the spin information is carried through the molecule by a propagation of spin polarization and the corresponding steric exchange effects.

There is the question of whether J-**OC**-PSP can also be applied within other quantum chemical approaches. Clearly, wavefunction methods that do not lead to reliable SSCCs are not attractive for using J-**OC**-PSP. For example, J-**OC**-PSP could be applied straightforwardly on the basis of CP-HF, but the analysis would be largely useless because of the poor SSCC values obtained with CP-HF. MCSCF and CCSD would be candidates for using the J-**OC**-PSP analysis provided that one expresses the corresponding wavefunctions in natural orbitals and repeat the calculation, which would of course increase the cost of the analysis substantially. Hence one can say that neither MCSCF nor CCSD is suitable to be run in connection with J-**OC**-PSP so that the analysis method is tightly bound to CP-DFT.

CONCLUSIONS

In this work, the requirements and a suitable strategy for the analysis of the spin–spin coupling mechanism have been derived. J-**OC**-PSP has been found to fulfill these requirements and to provide a hierarchical strategy that leads to additional information depending on the efforts that one makes in terms of additional selected orbital calculations. This has been demonstrated for some typical SSCC problems, for which J-**OC**-PSP provides satisfactory answers and in addition helps to correct or clarify misconceptions:

1. The simplified picture that the spin–spin coupling mechanism follows the path given by the chemical bonds, i.e. a path of maximum electron density connections,[83] is only true for the FC mechanism and in this case just for one- or two-bond SSCCs in a limited way. Even for the FC term, through-space mechanisms are more important than is generally realized and they can become dominant for three- and more-bond SSCCs.
2. Barfield's emphasis of rear-lobe interactions between orbitals[8,10] is fully confirmed as the major mechanism for through-space FC coupling over three bonds in ethane, four bonds in propane, etc. For example, the σ(CC) orbital in ethane has only a total contribution of 0.1 Hz to the vicinal SSCC ^3J(H,H).
3. The ^{3}FC(H,H) coupling in ethane depends much more strongly on the non-Lewis parts of the participating σ(CH) orbitals rather than the Lewis parts. This is in line with the original work of Karplus[3,4] and recent work by Esteban *et al.*,[76] but contradicts results obtained with the NJC-2 analysis.[65] The delocalization tails of the σ(CH) orbitals account nearly completely for the one-orbital coupling and for about 50% of the two-orbital coupling between the **H** nuclei. The coupling mechanism can be seen as a

'through-tail' mechanism that explains easily the influence of electronegative [contraction of the tail; smaller ^3J(H,H) values] or electropositive substituents [expansion of the tail; larger ^3J(H,H) values].[76]

4. The π FC coupling between the double bond units in polyenes is largely analogous to the 'through-tail' mechanism found for the vicinal HH coupling in ethane: the π orbitals transfer the spin information across the formal single bonds through their delocalization tails, which allow a formal single bond to be bridged both by single π orbital delocalization and by steric exchange interactions between adjacent π orbitals. The latter process is the dominant one.

With the J-**OC**-PSP methods we have for the first time a tool that provides a complete and detailed analysis of the NMR spin–spin coupling mechanism in terms of orbital contributions, Ramsey densities, and Ramsey energy densities. The method has already been applied in a successful way to one-bond SSCC,[42] the investigation of lone-pair effects, the dependence of the spin–spin coupling mechanism on electronegativity and polarizability of the coupling atoms,[42] the understanding of the Karplus relationship,[50] the role of the π electrons in the coupling mechanism,[43] the relationship between SSCC and bond order,[46,47] the experimental determination of NC coupling,[46] long-range coupling,[43] multipath coupling[48,79] and coupling across H-bonds,[38,49] to name just a few topics. The investigation of other topics (through-space coupling, coupling through multiple metal bonds, etc.) is under way.

Acknowledgments

Calculations were done on the supercomputers of the Nationellt Superdatorcentrum (NSC), Linköping, Sweden. D.C. thanks the NSC for a generous allotment of computer time. J.G. thanks Carl Tryggers Stiftelse for financial support.

REFERENCES

1. Grant DM, Harris RK (eds). *Encyclopedia of Nuclear Magnetic Resonance*, vols 1–8. Wiley: Chichester, 1996; and references cited therein.
2. Ramsey NF. *Phys. Rev.* 1953; **91**: 303.
3. (a) Karplus M, Anderson DH. *J. Chem. Phys.* 1959; **30**: 6; (b) Karplus M. *J. Chem. Phys.* 1959; **30**: 11.
4. Karplus M. *J. Am. Chem. Soc.* 1963; **85**: 2870.
5. Barfield M, Karplus M. *J. Am. Chem. Soc.* 1969; **91**: 1.
6. Pople JA, Santry DP. *Mol. Phys.* 1965; **9**: 311.
7. Pople JA, Bothner-By AA. *J. Chem. Phys.* 1965; **42**: 1339.
8. Barfield M, Chakrabarti B. *Chem. Rev.* 1969; **69**: 757.
9. Barfield M, Dean AM, Fallick CJ, Spear RJ, Sternhell S, Westerman PW. *J. Am. Chem. Soc.* 1975; **97**: 1482.
10. (a) Barfield M, Conn SA, Marshall JL, Miiller DE. *J. Am. Chem. Soc.* 1976; **98**: 6253; (b) Barfield M, Brown SE, Canada ED Jr, Ledford ND, Marshall JL, Walter SR, Yakali E. *J. Am. Chem. Soc.* 1980; **102**: 3355; (c) Barfield M. In *Encyclopedia of Nuclear Magnetic Resonance*, Grant DM, Harris RK (eds). Wiley: Chichester, 1996; 2520.
11. (a) Barfield M, *J. Am. Chem. Soc.* 1971; **93**: 1066; (b) Barfield M. *Mag. Res. Chem.* 2003; **41**: 344.
12. Barfield M, Sternhell S. *J. Am. Chem. Soc.* 1972; **94**: 1905.
13. (a) Barfield M, Spear RJ, Sternhell S. *J. Am. Chem. Soc.* 1971; **93**: 5322; (b) Barfield M, Spear RJ, Sternhell S, *J. Am. Chem. Soc.* 1975; **97**: 5160.
14. (a) Barfield M, Dingley AJ, Feigon J, Grzesiek S. *J. Am. Chem. Soc.* 2001; **123**: 4014; (b) Fierman M, Nelson A, Khan SI, Barfield M, O'Leary DJ. *Org. Lett.* 2000; **2**: 2077; (c) Grzesiek S, Barfield M, Cordier F, Dingley A, Feigon J, Nicholson LK. *Biochemistry* 2000; **39**: 89; (d) Dingley AJ, Masse JE, Peterson RD, Barfield M. *J. Am. Chem. Soc.* 1999; **121**: 6019.
15. (a) Pople JA, McIver JW, Ostlund NS. *J. Chem. Phys.* 1968; **49**: 2960; (b) Peralta JE, Ruiz de Azua MC, Contreras RH. *Theor. Chem. Acc.* 2000; **105**: 165.
16. (a) Kowalewski J. *Prog. Nucl. Magn. Reson. Spectrosc.* 1977; **11**: 1; (b) Kowalewski J. *Annu. Rep. NMR Spectrosc.* 1982; **12**: 81.
17. (a) Helgaker T, Jaszunski M, Ruud K. *Chem. Rev.* 1998; **99**: 293; (b) Fukui H. *Prog. Nucl. Magn. Reson. Spectrosc.* 1999; **35**: 267.
18. (a) Oddershede J. In *Methods in Computational Molecular Physics*, Wilson S, Diercksen GHF (eds). Plenum Press: New York, 1992; 303; (b) Wigglesworth RD, Raynes WT, Sauer SPA, Oddershede J. *Mol. Phys.* 1997; **92**: 77; (c) Wigglesworth RD, Raynes WT, Sauer SPA, Oddershede J. *Mol. Phys.* 1998; **94**: 851; (d) Enevoldsen T, Oddershede J, Sauer SPA. *Theor. Chem. Acc.* 1998; **100**: 275; (e) Wigglesworth RD, Raynes WT, Kirpekar S, Oddershede J, Sauer SPA. *J. Chem. Phys.* 2000; **112**: 3735.
19. (a) Laaksonen A, Kowalewski J, Saunders VR. *Chem. Phys.* 1983; **80**: 221; (b) Vahtras O, Ågren H, Jørgensen P, Jensen HJA, Helgaker T, Olsen J. *J. Chem. Phys.* 1992; **96**: 2118; (c) *J. Chem. Phys.* 1992; **97**: 9178.
20. Perera SA, Nooijen M, Bartlett RJ. *J. Chem. Phys.* 1996; **104**: 3290.
21. (a) Gauss J, Stanton JF. *Chem. Phys. Lett.* 1997; **276**: 70; (b) Auer AA, Gauss J. *J. Chem. Phys.* 2001; **115**: 1619.
22. Sychrovský V, Gräfenstein J, Cremer D. *J. Chem. Phys.* 2000; **113**: 3530.
23. (a) Helgaker T, Watson M, Handy NC. *J. Chem. Phys.* 2000; **113**: 9402; (b) Barone V, Peralta JE, Contreras RH, Snyder JP. *J. Phys. Chem. A* 2002; **23**: 5607; (c) Peralta JE, Barone V, de Azua MC, Contreras RH. *Mol. Phys.* 2001; **99**: 655; (d) Peralta JE, de Azua MC, Contreras RH. *Theor. Chem. Acc.* 2000; **105**: 165.
24. Contreras RH, Facelli JC. *Annu. Rep. NMR Spectrosc.* 1993; **27**: 255.
25. (a) Contreras RH, Peralta JE. *Prog. Nucl. Magn. Reson. Spectrosc.* 2000; **37**: 321; (b) Contreras RH, Peralta JE, Biribet CG, De Azua MC, Facelli JC. *Annu. Rep. NMR Spectrosc.* 2000; **41**: 55.
26. Contreras RH, Barone V, Facelli JC, Peralta J. *Annu. Rep. NMR Spectrosc.* 2003; **51**: 167.
27. (a) Engelmann AR, Contreras RH, Facelli JC. *Theor. Chim. Acta* 1981; **59**: 17; (b) Engelmann AR, Contreras RH. *Int. J. Quantum Chem.* 1983; **23**: 1033.
28. Diz AC, Giribet CG, Ruiz De Azua MC, Contreras RH. *Int. J. Quantum Chem.* 1990; **37**: 663.
29. Peralta JE, Contreras RH, Snyder JP. *Chem. Commun.* 2000; 2025.
30. (a) Perdew JP. In *Electronic Structure of Solids '91*, Ziesche P, Eschrig H (eds). Akademie-Verlag: Berlin, 1991; 11; (b) Perdew JP, Wang Y. *Phys. Rev. B* 1992; **45**: 13 244.
31. Becke AD. *J. Chem. Phys.* 1993; **98**: 5648.
32. Cremer D, *Mol. Phys.*, 2001; **99**: 1899.
33. (a) Polo V, Kraka E, Cremer D. *Mol. Phys.* 2002; **100**: 1771; (b) Polo V, Kraka E, Cremer D. *Theor. Chem. Acc.* 2002; **107**: 291.
34. (a) Polo V, Gräfenstein J, Kraka E, Cremer D. *Chem. Phys. Lett.* 2002; **352**: 469; (b) Polo V, Gräfenstein J, Kraka E, Cremer D. *Theor. Chem. Acc.* 2003; **109**: 22.
35. (a) Gräfenstein J, Kraka E, Cremer D. *J. Chem. Phys.* 2004; **120**: 524; (b) Gräfenstein J, Kraka E, Cremer D. *Phys. Chem. Chem. Phys.* 2004; **6**: 1096.
36. (a) Peralta JE, Scuseria GE, Cheeseman JR, Frisch MJ. *Chem. Phys. Lett.* 2003; **375**: 452; (b) Helgaker T, Jaszuński M, Ruud K, Górska A. *Theor. Chem. Acc.* 1998; **99**: 175; (c) Provasi PF, Aucar GA, Sauer SPA. *J. Chem. Phys.* 2001; **115**: 1324.
37. Sychrovsky V, Vacek J, Hobza P, Zidek L, Sklenar V, Cremer D. *J. Phys. Chem. B* 2002; **106**: 10 242.
38. Tuttle T, Wu A, Kraka E, Cremer D. *J. Am. Chem. Soc.* 2004; **126**: 5093.
39. Wu A, Cremer D, Auer AA, Gauss J. *J. Phys. Chem. A* 2002; **106**: 657.
40. Wu A, Cremer D. *Int. J. Mol. Sci.* 2003; **4**: 159.
41. Wu A, Cremer D. *J. Phys. Chem. A* 2003; **107**: 1797.

42. Wu A, Gräfenstein J, Cremer D. *J. Phys. Chem.* 2003; **107**: 7043.
43. Gräfenstein J, Tuttle T, Cremer D. *J. Chem. Phys.* 2004; **120**: 9952.
44. Gräfenstein J, Cremer D. *Chem. Phys. Lett.* 2004; **383**: 332.
45. Gräfenstein J, Cremer D. *Chem. Phys. Lett.* 2004; **387**: 415.
46. Cremer D, Kraka E, Wu A, Lüttke W. *Chem. Phys. Chem.* 2004; **5**: 349.
47. Gräfenstein J, Kraka E, Cremer D. *J. Phys. Chem. A.* 2004; **108**: 4520.
48. Wu A, Cremer D. *Phys. Chem. Chem. Phys.* 2003; **5**: 4541.
49. Tuttle T, Gräfenstein J, Wu A, Kraka E, Cremer D, *J. Phys. Chem. B* 2004; **108**: 1115.
50. Gräfenstein J, Tuttle T, Cremer D. *J. Am. Chem. Soc.* submitted.
51. Itagaki T, Saika A. *J. Chem. Phys.* 1979; **71**: 4620.
52. Kowalewski J, Laaksonen A, Roos B, Siegbahn P. *J. Chem. Phys.* 1980; **71**: 2896.
53. Laaksonen A, Kowalewski J, Saunders VR. *Chem. Phys.* 1983; **80**: 221.
54. Sekino H, Bartlett RJ. *J. Chem. Phys.* 1986; **85**: 3945.
55. Fukui H. *J. Chem. Phys.* 1976; **65**: 844.
56. Malkin VG, Malkina OL, Salahub DR. *Chem. Phys. Lett.* 1994; **221**: 91.
57. Malkina OL, Salahub DR, Malkin VG. *J. Chem. Phys.* 1996; **105**: 8793.
58. Dickson RM, Ziegler T. *J. Phys. Chem.* 1996; **100**: 5286.
59. Malkin VG, Malkina OL, Casida ME, Salahub DR. *J. Am. Chem. Soc.* 1994; **116**: 5898.
60. Jameson CJ. *Multinuclear NMR*. Plenum Press: New York, 1987.
61. Oddershede J. In *Nuclear Magnetic Resonance. Specialist Periodical Report*, vol. 18, Webb GA (ed). Royal Society of Chemistry: Cambridge, 1988; 98.
62. Boys SF. *Rev. Mod. Phys.* 1960; **32**: 296.
63. (a) Carpenter JE, Weinhold F. *J. Mol. Struct. (Theochem)* 1988; **46**: 41; (b) Reed AE, Weinstock RB, Weinhold F. *J. Chem. Phys.* 1985; **83**: 735; (c) Reed AE, Curtiss LA, Weinhold F. *Chem. Rev.* 1988; **88**: 899.
64. Kohn W, Sham LJ. *Phys. Rev. A* 1965; **140**: 1133.
65. Wilkens SJ, Westler WM, Markley JL, Weinhold F. *J. Am. Chem. Soc.* 2001; **123**: 12 026.
66. Engelmann AR, Scuseria GE, Contreras RH. *J. Magn. Reson.* 1982; **50**: 21.
67. (a) Fukui H, Tsuji T, Miura K. *J. Am. Chem. Soc.* 1981; **103**: 3652; (b) Fukui H, Miura K, Ohta K, and Tsuji T. *J. Chem. Phys.* 1982; **76**: 5169.
68. Schaefer T. In *Encyclopedia of Nuclear Magnetic Resonance*, Grant DM, Harris RK (eds). Wiley: Chichester, 1996; 4571.
69. Gräfenstein J, Tuttle T, Cremer D. *Chem. Eur. J.* submitted.
70. Becke AD. *Phys. Rev. A* 1988; **38**: 3098.
71. Lee C, Yang W, Parr RP. *Phys. Rev. B* 1988; **37**: 785.
72. (a) Huzinaga S, *Approximate Atomic Wave Functions*. University of Alberta: Edmonton, 1971; (b) Kutzelnigg W, Fleischer U, Schindler M. In *NMR–Basic Principles and Progress*, vol. 23. Springer: Heidelberg, 1990; 165.
73. Gray DL, Robiette AG. *Mol. Phys.* 1979; **37**: 1901.
74. Kraka E, Gräfenstein J, Filatov M, He Y, Gauss J, Wu A, Polo V, Olsson L, Konkoli Z, He Z, Cremer D. *COLOGNE 2003*. Göteborg University: Göteborg, 2003.
75. Altona C. In *Encyclopedia of Nuclear Magnetic Resonance*, Grant DM, Harris RK (eds). Wiley: Chichester, 1996; 4909.
76. Esteban AL, Galache MP, Mora F, Díez E, Casanueva J, Fabián JS, Barone V, Peralta JE, Contreras RH. *J. Phys. Chem. A* 2001; **105**: 5298.
77. Günther H. *NMR-Spectroscopy*. Georg Thieme: Stuttgart, 1983; p 114.
78. Günther H. *NMR-Spectroscopy*. Georg Thieme: Stuttgart, 1983.
79. Gräfenstein J, Cremer D. *J. Phys. Chem.*, submitted.
80. Jameson CJ, Buckingham AD. *J. Chem. Phys.* 1980; **73**: 5684.
81. Malkina OL, Malkin VG. *Angew. Chem.* 2003; **115**: 4471.
82. Soncini A, Lazzeretti P. *J. Chem. Phys.* 2003; **118**: 7165.
83. (a) Cremer D, Kraka E. *Angew. Chem.* 1984; **96**: 612; *Angew. Chem., Int. Edt. Engl.* 1984; **23**: 627; (b) Cremer D, Kraka E. *Croat. Chem. Acta* 1984; **57**: 1259; (c) Kraka E, Cremer D. In *Theoretical Models of Chemical Bonding, Part 2: the Concept of the Chemical Bond*, Maksic ZB (ed). Springer: Heidelberg, 1990; 453.